

Engineering of Microfabricated Ion Traps and Integration of Advanced On-Chip Features

Zak David Romaszko, Seokjun Hong, Martin Siegele, Reuben Kahan Puddy, Foni Raphaël Lebrun-Gallagher, Sebastian Weidt, Winfried Karl Hensinger*

Sussex Centre for Quantum Technologies, Department of Physics and Astronomy, University of Sussex, Brighton, BN1 9QH, United Kingdom

Abstract

Trapped atomic ions are a proven and powerful tool for the fundamental research of quantum physics. They have emerged in recent years as one of the most promising candidates for several practical technologies including quantum computers, quantum simulators, atomic clocks, mass spectrometers and quantum sensors. Advanced fabrication techniques, taken from established and nascent disciplines, are being deployed to create novel, reliable devices with a view to large scale integration and commercial compatibility. This review will cover the fundamentals of ion trapping before proceeding with a discussion of the design of ion traps for the aforementioned applications. We will analyse current microfabrication techniques that are being utilised, as well as various considerations which motivate the choice of materials and processes. Finally, we discuss current efforts to include advanced, on-chip features into next generation ion traps.

1. Introduction

The trapping of atomic ions within confining electric fields in vacuum was first conceived of, and demonstrated by, Wolfgang Paul and Hans Georg Dehmelt, securing them a share of the Nobel prize in 1989 [1], [2]. An ion isolated in this way can be extremely well decoupled from its environment and thus be cooled to record low temperatures using laser techniques such as those developed by David Wineland [3]. The extreme isolation and low thermal energy mean that the energy levels of the ion are highly stable and well resolved, with quantum states having been observed to remain coherent over several minutes [4], [5]. This, along with the ability to prepare and detect the quantum states and generate high fidelity entanglement between trapped ions, make trapped ion systems a prime candidate for use in a wide range of fields that require the precise control of well-defined quantum systems. These include atomic clocks [6], quantum sensors [7], quantum simulators [8]–[11], mass spectrometers [12]–[14] and quantum computation [15], [16].

The Paul trap uses oscillating (RF) voltages to create potential minima in up to three dimensions (see Figure 1.1), which, when combined with DC fields, are able to manipulate an ion's position [1]. With many of the applications of trapped ions, comes the desire to significantly increase the number of ions while maintaining, and in some cases increasing, precise control over the position of individual ions. Quantum computing is a good example where many approaches to scalability require such a level of control [17]–[19]. This requires a significant reduction in the size and an increase in the number of control electrodes, making the early type of Paul traps, consisting of mechanically machined 3D electrode structures, unsuitable [20]. The use of microfabrication methods allows for the realisation of the required feature sizes, reproducibility and mass producibility needed for such devices. This led to a proposal in 1999 which used laser-machined, gold-on-alumina wafers to make ion traps [21]. This was followed by monolithic ion microchips which were lithographically patterned that were first demonstrated in 2006 [22], [23]. Whilst quantum computing provided the first motives for utilising microfabricated devices in ion traps, other trapped ion technologies have these developments to their advantage. For instance, lithographic methods contributed to the realisation of a compact ion trap

*Z.Romaszko@sussex.ac.uk

package for portable atomic clocks [24], [25] and also quantum simulations in 2D lattices with micron-scale inter-ion distance [26], [27].

These ‘trap-on-chip’ devices utilise established fabrication techniques from the semiconductor and micro-electro-mechanical system (MEMS) industries to realise micron scale architectures in both 2D (surface traps) [23], [28] and 3D configurations [22], [29]. Another set of well-established techniques, which is also highly prevalent in modern electronics, comes from complementary metal–oxide–semiconductor (CMOS) technology and has been used to successfully fabricate an ion trap [30]. These methods have allowed the creation of reliable ion traps using established processes, giving trapped ions a prominent position in quantum technologies.

In addition to the miniaturisation of the ion trap, the integration of peripheral components, such as photodetectors [31] and digital to analogue converters (DACs) [32], into the ion trap is also of great interest. Integration of these components allows the creation of compact devices and stand-alone trap modules and can also offer the potential to reduce electrical noise [33]. In addition, the integration of peripheral components may be critical for large scale quantum computing with trapped ions where stand-alone modules are a key ingredient to scalability [18], [19].

To create a sufficiently large quantum computer, the ability to connect between modules is required. Two methods that address the connectivity between modules have been proposed. One scheme, proposed by Monroe *et al.* [18], [34], uses photons, emitted by ions on separate modules, to initiate inter-module entanglement. Another method, proposed by Lekitsch *et al.* [19], relies on shaping electrodes in such a way that when neighbouring modules are closely aligned, ions can be transported from one module to another using electric fields.

This paper reviews the state-of-the-art of microfabricated ion traps including efforts to integrate advanced features such as optical components and electrical devices. In Section 2, the basic principles of ion trap electrode design are given. Conventional microfabrication techniques applied to ion traps are detailed in Section 3. Section 4 describes current research into integration of advanced features into an ion trap chip. Finally, Section 5 summarises this review with a discussion of the technological issues expected in the coming years. For further discussion of ion trap supporting hardware, and other ion trap fabrication reviews, we suggest references. [35]–[40].

BOX 1: Evolution of ion trap structures

The first Paul trap (Figure 1.1(a)) used hyperbolic electrodes in a 3D configuration [1], and with this structure, many fundamental experiments including the isolation of single ion [41] and the demonstration of a quantum logic gate [42] have been demonstrated. However, this structure could only trap a single ion without having significant micromotion, which limited the measurement accuracy of atomic resonances. To address this limitation, the linear Paul trap was developed [43], [44]. These traps consist of four machined rods assembled in parallel to confine ions radially and two end cap electrodes to axially confine ions [45], as shown in Figure 1.1(b). One of the most important characteristics of this linear trap is that ions in the same string share their motional modes. This feature gave rise to the first proposal of trapped ion based qubit operations by Cirac and Zoller [15], which was experimentally demonstrated in 2003 [46] in a linear Paul trap.

The 4-rod trap can have high voltages (>1 kV) applied to it, which allows the creation of deep trapping potentials whilst maintaining stable parameters. The electrodes are also at a sufficiently large distance from the ions to minimise the effects of electrical noise from the electrodes. Segmenting these rods

allows axial control of ions along a string. Owing to these strengths, 4-rod Paul traps are widely used in experiments with ion chains in situations that do not require microfabricated devices [46]–[49]. Notwithstanding the numerous successes of these ion traps, precise control is required for operations such as ion crystal separation, which could only be allowed by more electrodes of smaller sizes. To address this, lithographic techniques from the semiconductor industry were used to fabricate ion traps [22], [50]. These ion trap reproduced the 4-rod structure on a micron-scale, but the vertical distance between the electrodes was inevitably limited by the technical capability of thin film processes. As a solution that may offer advantages for general scalability, Chiaverini *et al.* [28] proposed (and Seidelin *et al.* [23] subsequently demonstrated) a direct projection of four rods onto a single plane resulting in a five-wire geometry. This trap lays two radio-frequency (RF) electrodes and three ground electrodes alternately, as shown in Figure 1.1(c). This chip structure is referred to as a “surface electrode trap” (or “surface trap”) and has become the most widely used geometry for microfabricated ion trap chips. Advances in fabrication technologies have allowed more complex designs to be pursued [17], [26], [27], [29], [51].

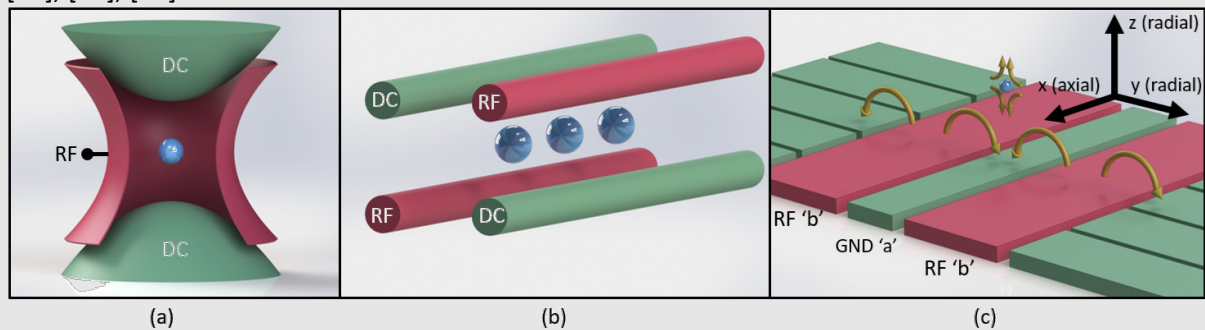


Figure 1.1. Evolution of electrode structure of ion traps with ions shown in dark blue. **(a)** The initial ion trap design which consists of a hyperbolic-structured RF electrode and two end-cap electrodes. **(b)** The linear trap with four linear rods assembled in parallel and two end-cap electrodes (not shown in this diagram). **(c)** The surface ion trap chip in the conventional five-wire geometry where ‘a’ and ‘b’ represent the widths of the ground and RF electrodes respectively. The yellow arrows indicate the electric field when the RF electrode has a positive voltage applied.

Modern trap designs have, in part, been motivated by the creation of a trapped ion quantum computer. Concepts for trapped ion quantum computers were initially suggested by Wineland *et al.* [52] and Cirac *et al.* [53]. Following this, Kielpinski *et al.* [17] proposed an architecture in which ions are shuttled around a 2D array using time dependant electric fields generated by nearby electrodes. The array consists of regions that have specific functions, such as gate operations or ion storage, which are connected by linear and junction sections.

2. Ion Trap Geometries

This section will discuss basic ion trap geometries for top layer electrode design, as well as the geometrical considerations for ion transport and advanced ion trap designs. The basics of ion trapping are covered in Box 2.

2.1 Basic principles of five-wire geometry

Figure 1.1(c) shows a simplified planar view of a surface ion trap in a symmetric, five-wire geometry. An RF voltage is applied to a pair of linear electrodes while all the other electrodes are held at RF ground. The ponderomotive potential generated by the RF voltage confines ions parallel to the z axis at a height given by the widths of the RF and central ground electrode. Assuming infinitely long rails, the zero potential line from the RF, the RF nil, can be expanded along the longitudinal direction, and

the axial position of the ions can be determined by static electric fields only. To generate the static electric field required for trapping or shuttling the ions in the axial direction, a calculated, direct-current (DC) voltage set is applied to the segmented electrodes [54], [55].

The five-wire electrode geometry of surface ion traps has been analytically modelled in numerous studies [28], [56], [57] including the modelling of electrostatics due to gaps between electrodes [58]. The width of the RF and ground ('a' and 'b' respectively, as shown in Figure 1.1(c)) electrode in a gapless, five-wire geometry can be used to determine the trap depth, ψ_E , and ion height, h_{RFnil} [56];

Equation 1

$$\psi_E = \frac{e^2 V^2}{\pi^2 m \Omega^2} \frac{b^2}{(a + b)^2 + (a + b)\sqrt{2ab + a^2}},$$

Equation 2

$$h_{RFnil} = \frac{\sqrt{2ab + a^2}}{2},$$

Where the trap depth is the difference in the ponderomotive potential between the RF nil and the escape point, and Ω , e , m , and V indicate the RF drive frequency in Hz, elementary charge in Coulombs, ion mass in kilograms, and RF voltage amplitude in volts, respectively.

For long ion lifetimes, a high trap depth is required. For a low ion motional heating rate, a large ion-electrode distance is wanted. These parameter optimisations cannot be achieved simultaneously (especially given differing scaling laws), and compromises should be determined by considering the constraints given by one's experimental setup [59], [60]. Nizamani *et al.* [60] analytically demonstrated that a ratio of RF and ground rails widths of $b/a = 3.68$, provided a maximised trap depth. However, this wide ratio, increases the distance between the outer DC electrodes and the trapped ions, thus reducing DC confinement. A solution to this replaces the central ground electrode, with segmented DC electrodes allowing for a minimised ion-electrode distance [55], however, depending on fabrication constraints, this is not always achievable. This balancing act is common place in ion trap design and can depend heavily on purpose of the experiment and voltage range available on the electrodes. The longitudinal (axial) direction is not usually considered during simple, RF electrode design, since its properties are mainly determined by DC voltages.

2.2 Rotation of principle axes

In a typical experimental setup with a surface ion trap, laser paths are limited to the directions parallel or perpendicular (through a vertical hole penetrating the substrate [55]) to the surface of the trap chip. To be able to effectively Doppler cool an ion in all motional directions (principal axes), the laser path must interact with all the principal axes. This is achieved by rotating the principal axes of motion (Figure 2.1). The rotation can be achieved by tilting the total electric potential at the ion position. The rotation angle can be calculated from the eigenvectors of the Hessian matrix of the total electric potential. To tilt the potential, there are two commonly used methods. The first approach uses RF rails of different widths, which rotates the potential [23], [57], [61]. The second method is achieved by applying asymmetric DC voltages to 'rotation' electrodes. Rotation electrodes can be introduced by replacing the central ground electrode in a 5-wire geometry with two electrodes which occupy the same space, creating a 6-wire geometry. As this will move the ion out of the RF nil, additional voltages are applied to the control electrodes (Figure 2.1) and are required to compensate for non-zero fields

[54], [62]. Asymmetric RF electrodes were initially used for surface traps, until proposals were made to rotate the principal axis using DC voltages instead. The use of asymmetric DC voltages applied to these electrodes, became a popular approach since it could easily achieve a $\theta = 45^\circ$ rotation angle, allowing for all degrees of freedom to be addressed by a planar laser path [54].

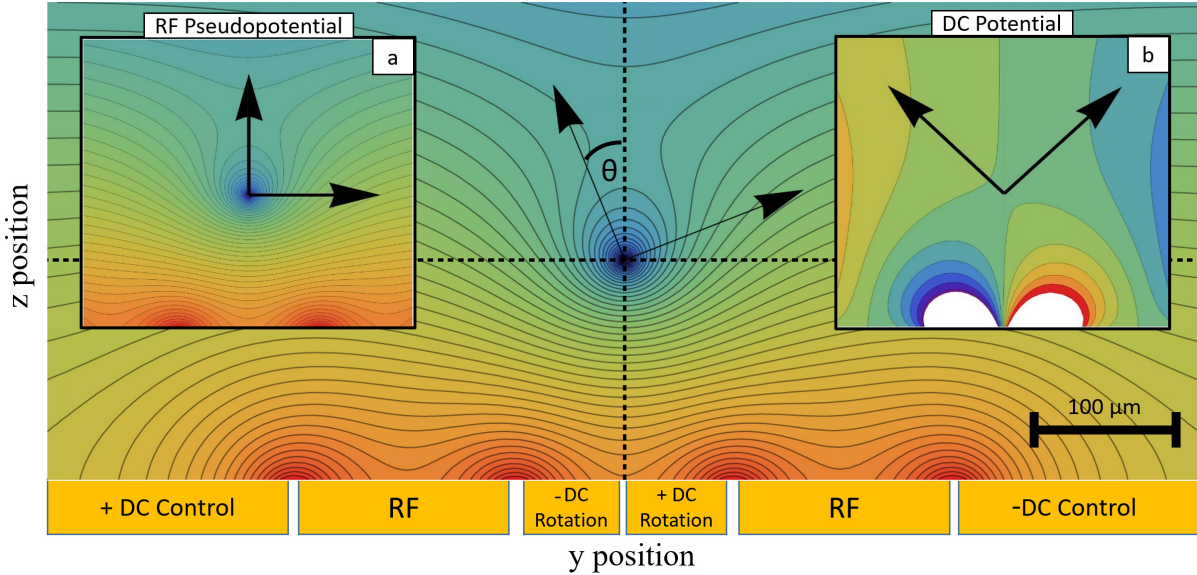


Figure 2.1. Method of rotating the principal axis by angle, θ using a 6 wire surface trap design [54]. The arrows show the principal axis in the radial directions. The relative sign of the voltage to achieve the rotation is indicated on the electrodes. The scale indicates typical dimensions of the electrodes, however, these can vastly differ depending on the wanted ion height and trap parameters. The central contour plot shows the total potential, ϕ_{tot} created from the superposition of (a) the RF Pseudopotential and (b) the DC rotation potential created by asymmetric voltages on DC electrodes.

2.4 Design and optimisation of geometries for ion transport and quantum simulation

Some trapped ion uses, especially quantum computation, require the ability to move ions in a trapping potential such that certain operations are only performed on particular ions. Generally speaking, there are four types of operations required; linear shuttling, junction shuttling and separation and combination of ion crystals. These operations are carried out using time-dependent voltages applied to control electrodes which are located on the trap. The optimal geometries of these electrodes (in relation to electrode-ion distance) for operations such as linear shuttling and ion crystal (re)combination have been discussed in [56], [60]. These transport operations have been reliably shown with high fidelity [63]–[67], based on the theoretical work presented in [68]–[70].

Whilst linear shuttling operations can be performed using the types of ion traps previously discussed, junction shuttling, and by extension, 2D ion trap planes, require several modifications. Arrays of trapping zones arranged in a 2D plane were first proposed in [17] and expanded towards an industrial blueprint for quantum computing in [19]. The first realisation of ion transport through a junction was demonstrated in a T-junction ion trap array [71]. Subsequent studies identified optimal geometries for ion trap arrays where linear regions are connected to others via junction nodes [72], [73]. At the centre of a junction node, three (T [71] or Y-junction [51]) or four (X-junction [74]) branches of linear rails join together, making the infinitely long rail assumption no longer valid. Consequentially, the uniform extension of the RF field along the axial direction terminates at this point (Figure 2.2). Changes in the ion's secular frequencies or being transported over a gradient in the pseudopotential, such as

that caused by a junction, can cause motional heating of the ion [74], [75]. To minimise these effects, geometry optimisations have been introduced to improve junctions [73], [76], [77]. Most of the optimised geometries are created using iterative optimisation methods such as a genetic algorithm. Using these designs, a number of successful experimental results of junction transport have been reported [51], [74], [78], achieving 10^5 consecutive transports with Doppler cooling and 65 without [76]. Furthermore, Kaufmann *et al.* [67] have shown preservation of quantum information during trapped ion transport with 99.9994% state fidelity.

Whilst the previous designs are used for generic ion traps, for quantum simulations, two-dimensional ion lattices of stationary ions (with small inter-site distances) can be beneficial. Ion traps to create these lattices have been successfully fabricated as mechanical structures [59], and subsequently as a microfabricated ion trap chip [26]. Schmied *et al.* [79] presents a useful tool for creating geometries required for close lattice sites. Using this tool, lattice geometries have been fabricated with close, inter-site distance and multiple degrees of freedom per site [27], [80]. This tool has also been used to investigate bi-layer ion traps which can be used to achieve stronger coupling between adjacent sites than with lattices fabricated on surface ion traps [81].

2.5 Numerical Simulation Tools

As the scope of ion trap experiments have evolved, so have the requirements of the ion traps themselves. Such requirements include the introduction of vertical holes penetrating the substrate for additional access of laser light or atomic flux to the ion position [82], as well as the split rotation rails and the junction geometries already discussed in the previous part of this section. For those geometries, analytical methods are no longer viable, therefore numerical simulations of electric fields are essential for designing electrodes. In the early years of surface traps, the boundary element method (BEM) was used to simulate simple geometries with a single electrode layer [83], owing to the available computational resources. Advances in computational power have meant that the finite element method (FEM) has become a viable simulation tool and geometries with greater complexity, including structures for oscillating magnetic field gradient schemes (see Section 4.1), are routinely modelled and optimised using this method [77], [84], [85]. Figure 2.2 shows an x-junction device which has been optimised to reduce the pseudopotential gradient which in turn reduces the motional heating rate, \dot{n} , through ion transport [76].

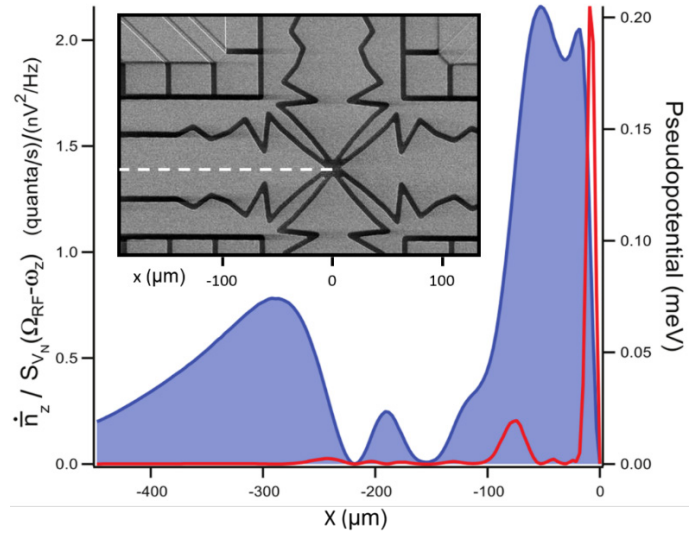


Figure 2.2. Optimised x-junction electrode geometry at the junction centre (inset image) to reduce the ratio of the motional heating, \dot{n} , to the spectral voltage noise, S_{V_N} (red line). It is expressed as the quantity \dot{n} / S_{V_N} to normalise against material and electronics dependent noise. This ratio provides a measure of the gradient in the pseudopotential and local secular frequency both of which determine the motional heating during ion transport [74]. The blue shaded line shows the RF pseudopotential along the transport direction. The trap potential is evaluated for a ^{40}Ca ion with $V = 91 \text{ V}_{\text{rms}}$ and $\Omega = 2\pi \times 58.55 \text{ MHz}$. Figure taken from [76] and modified for continuity.

BOX 2: Ion trapping 101

A simplified in-vacuum setup of a typical, microfabricated, surface ion trap experiment is shown by Figure 2.3.

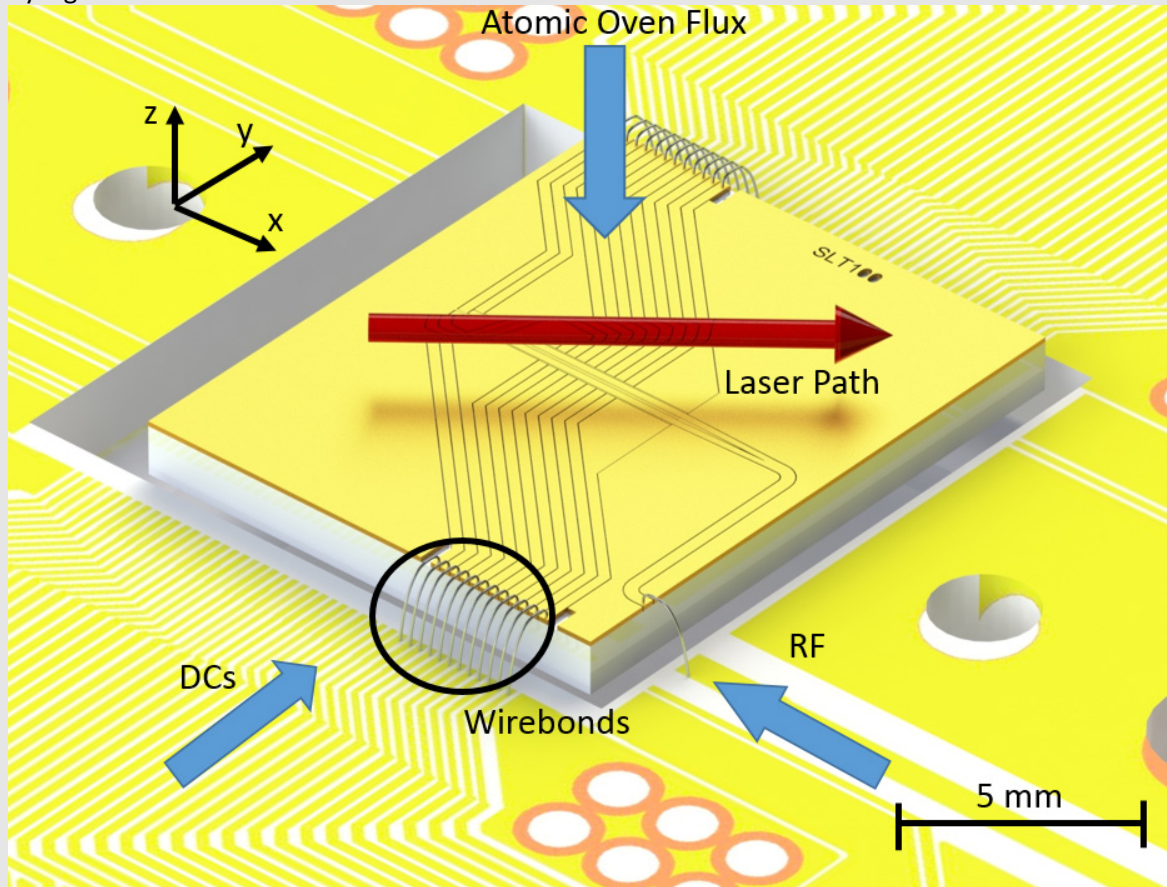


Figure 2.3 – A typical ion trap experiment setup. Ions are trapped in an ultra-high vacuum chamber with feedthroughs to connect the ion trap to supporting electronics and viewports for optical access.

By applying an RF voltage to the ion trap, one is able to create a trapping potential. DC voltages are applied to electrodes, creating a static field, and are used to confine the ion in the axial direction [1]. By adding time dependence to the electrode's voltage, ion transport operations can be realised. This can be expressed as,

Equation 3

$$\varphi_{tot}(x, y, z, t) = \varphi_{DC}(x, y, z) + \varphi_{RF}(x, y, z) \cos(\Omega t),$$

where φ_{tot} , φ_{DC} and φ_{RF} is the total, DC and RF potential respectively and Ω is the frequency at which RF is being driven.

The equations of motion for a particle in a Paul trap are given by,

Equation 4

$$\ddot{x} + \frac{e}{mr_0^2} (\varphi_{DC} - \varphi_{RF} \cos(\Omega t)) x = 0.$$

These equations follow that of the Mathieu equations which have the form

Equation 5

$$\frac{d^2 i}{d\zeta^2} + (a_i - 2q_i \cos(2\zeta)) i = 0,$$

where a_i and q_i are the stability parameters in a direction, i . Only a small subset of these parameters are stable which are given by Floquet theorem [86]. In the regime where $1 > q_i \gg a_i$, the ion's motion can be characterised in two ways, 'secular motion' and 'micromotion'. The secular motion is the motion due to the curvature of the electric potential. This motion is often used to implement spin-motion coupling [87]. Micromotion is an often unwanted part of the ion's motion and can be split into two forms; intrinsic and extrinsic micromotion. The latter is caused when the ion is not in the RF nil (caused by an external field contribution) and hence is subject to an additional, oscillatory component of motion. This can be compensated for by moving the ion to the RF nil. Intrinsic micromotion is caused by the ion's secular motion causing an effective offset to the RF nil in which the ion moves with an additional motion at the drive frequency Ω . This occurs even at the RF nil and cannot be compensated for entirely. For greater discussion into the motion of trapped ions, the authors recommend Leibfried *et al.* [88].

An atomic oven with a small aperture creates a flux of atoms parallel to the trap surface [89] during which process a laser is used to ionise the atoms [90]. The atomic flux can also lead to unwanted surface coating, and many efforts have been made to reduce this such as loading through a hole in the trap itself [51].

To initially cool the ion, Doppler cooling is employed [91]. When Doppler cooling, all 3 directions of motion must be considered to effectively cool the ion. To cool the in-plane directions of motion, the laser is typically positioned at a 45° angle with respect to the planar motion, to have cooling components acting in both 'x' and 'y' motion. The 'z' motion can be effectively cooled by rotating the principal axis using the methods discussed in Section 2.2. Additional lasers and laser paths may be required to perform laser based quantum logic operations [92].

The final consideration for ion trapping is optical access to the ion. Wirebonds are often used to connect the trap to a supporting printed circuit board (PCB). If the wirebonds are in the path of a laser, unwanted scattering will occur, which will drastically affect the ability to perform experiments. Scattering also occurs due to the divergence of a planar laser beam scattering off the surface of the trap. Some surface ion traps have been especially developed to reduce this scattering by including an optical access hole which allows laser access through the trap [62]. To image the ion, external optics, combined with charged-coupled devices (CCDs) and photo-multiplier tubes (PMTs) are employed. These sensors and optics are typically outside the vacuum system, however efforts are being made to integrate the required technology for the detection of ions into the ion trap structure (see Section 4.2).

3. Ion Trap Microfabrication Techniques

This section covers material considerations as well as the fabrication processes required for ion trap chips.

The semiconductor industry revolutionised the creation of miniature, electronic devices using patterned conducting and insulating materials, with the most common example being CMOS. Key to this success are highly reliable and reproducible processes using well established fabrication facilities (foundries). Microfabricated ion traps have been created which use these foundries [30], [32]. However, as will be outlined in Section 3.1, some ion trap specific requirements which necessitate structures which do not use established processes (such as formation and subsequent patterning of thick dielectric layers) or materials (such as gold and copper) are not permitted inside many foundries. As a result, modern ion trap fabrication borrows many techniques from across microfabrication, such as MEMS, with the eventual goal of achieving reproducible processes such as those used in CMOS.

3.1 General considerations for the microfabrication of ion trap chips

Critical features which should be addressed when designing ion trap chip structures and the required fabrication processes are as follows.

1. The electrodes should be able to sustain a RF voltage suitable for that ion species (heavier ions require larger voltages). A higher RF voltage allows trapping of ions farther from the chip surface, reducing the effects of the electrical field noise and laser scattering from the chip surface. In addition, higher voltages can allow for higher trap depths and secular frequencies.
2. Coupling of the RF field into the substrate should be minimised to prevent power loss and heating of the device [72].
3. The area of dielectric exposed to the trapped ions should be minimised. In general, any dielectric should be sufficiently shielded such that electric fields from trapped charges on the dielectric, are not felt by the ion. This is because factors such as ultraviolet (UV) lasers incident on dielectric surfaces can generate time-varying, stray charges in the dielectric [93]–[95], which in turn cause unwanted, time-dependent, ion displacements.
4. All the materials, including various deposited films, should be compatible with ultra-high vacuum (UHV) environments. The chip should also be able to withstand processes required to achieve UHV such as baking and cryogenic temperatures.
5. There must be clear optical access between lasers sources, detectors and the ions. This for example, requires that wirebonds do not impede the optical path.
6. Exposed surfaces should be contaminant free to the greatest extent to reduce anomalous heating of ions [96], [97]. In addition, a lower surface roughness reduces unwanted laser scattering and has been suggested to reduce anomalous heating at cryogenic temperatures [98].

3.2 Substrate materials

Designing a fabrication process for ion trap chips starts with the selection of layer materials, since the number and dimensions of thin film layers can drastically change the complexity of the whole process. Dielectric and conductive (or semi-conductive) substrates have their own distinct advantages and disadvantages. Use of dielectric substrates allows for a very simple fabrication process as well as low power loss and heat in the substrate. However, accurate bulk micromachining of dielectric substrates for introducing vertical penetration holes and buried metal layers can be difficult. Another concern is that of exposed dielectric surfaces can trap charges, causing stray fields [93].

Silicon is the most widely used material in modern semiconductor technology and has the advantage of utilising most processes that are not compatible with insulating substrates. It is, however, very lossy in the mid-range resistivity (10^2 - 10^4 Ω cm) for RF frequencies [99]. To compensate this, the simplest and most widely used method is to place an additional metal layer referred to as a 'ground plane' (M1, Figure 3.1) between the RF electrode and the substrate. Although this adds complexities to the fabrication of silicon ion trap chips, as detailed in the next subsection, it is widely adopted since it almost guarantees the successful shielding of the substrate from RF dissipation. Another approach is to use very high or very low resistive substrates [100]. In this case, the temperature dependence of the silicon resistivity should be considered - at cryogenic temperatures, silicon can even act as an insulator [101].

3.3 Standard fabrication processes for ion traps

Figure 3.1 shows a typical fabrication process of a silicon based, surface ion trap chip, which consists of a ground layer (M1), an electrode layer (M2), and two dielectric layers (D1 and D2) that are used to electrically isolate the conducting layers and the substrate. When using an insulating substrate, a simple ion trap can be created using M2 only and its formation is similar to that of M2 described in this section. The process starts with the deposition of a dielectric layer on the silicon substrate, which insulates the ground plane from the substrate. A 1-2 μm layer of either SiO_2 or SiN_x is used for this and is typically grown using plasma enhanced chemical vapour deposition (PECVD) or as a thermal oxide. A ground plane, M1, is deposited on the D1 layer (Figure 3.1(a)) using any UHV compatible conductive material such as Au, Al, Cu, etc. This is commonly a 1-2 μm layer, either sputtered or evaporated onto the device. When developing chips with vertical interconnect access (VIAs) to improve electrode routing, these thin insulating and conducting layers can be stacked multiple times [102]. Since high RF voltages applied between the electrodes and ground plane are desirable in surface ion traps, the D2 layer separating the two metal layers should therefore be thick, so as to maximise the voltage at which electrical breakdown occurs. Thus, the thickness of the D2 layer is generally on the order of 10 μm , with the deposition and etching of this layer usually being the most difficult steps throughout the entire ion trap fabrication (Figure 3.1(b)). This is because such vertical dimensions are generally not covered by conventional semiconductor processes, which also limits the material choice for the dielectric layer to PECVD SiO_2 or SiN_x . Bautista-Salvador *et al.* [103] demonstrated a polymer-based, spin-on dielectric for ion trap fabrication, which allowed for thick dielectric layers. Deposition of the top metal layer (M2) can be performed by using conventional microfabrication processes including electroplating, sputtering, evaporation (Figure 3.1(c)) and can be patterned using plasma dry-etching (Figure 3.1(d)). Since the top layer is directly exposed to the trapped ions, more factors should be considered when selecting the electrode material. Gold is one of the most widely used materials for the top metal layer owing to its extremely low oxidisation rate. However, since gold is not compatible with many conventional microfabrication techniques, it is also possible to deposit a thin gold layer on aluminium electrodes as a final step [104]. The final step etches the dielectric layer in both vertical and lateral directions to reduce the effect of charges trapped on the dielectric surface. The vertical etching of the thick dielectric layer (Figure 3.1(e)) uses the electrode pattern as a mask, and reactive ion etch (RIE) to etch. This is followed by isotropic wet or gas etching of the dielectric sidewalls (Figure 3.1(f)), which helps to minimise the exposure of the ions to trapped charges [62].

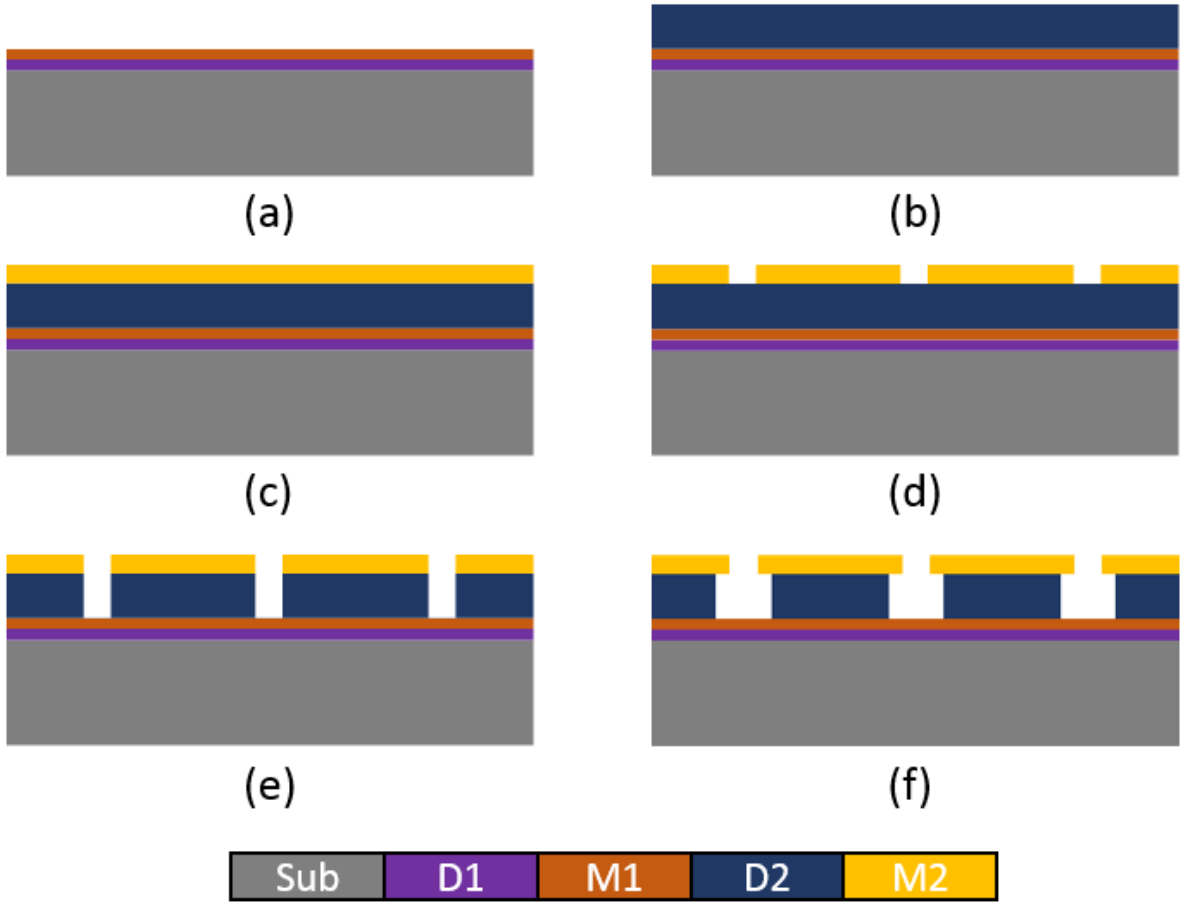


Figure 3.1. A conventional fabrication process flow of a surface ion trap chip. **(a)** Forming a ground plane and an insulating layer that isolates the ground plane and the substrate. **(b)** Deposition of a thick ($\sim\mu\text{m}$'s) dielectric layer. **(c)** Forming a metal layer on the dielectric. **(d)** Etching of the metal layer to define the electrode patterns. **(e)** Subsequent etching of the thick dielectric layer. **(f)** Isotropic etching of the dielectric pillars from the sidewalls to reduce the area of dielectric sidewalls exposed to the ion.

The fabrication methods described here are commonly used to implement a silicon-based ion trap chip. Microfabricated ion traps can also be fabricated by many different, additional processes not discussed in this review [35], [38]. Furthermore, fabrication processes have been optimised for specific capabilities, such as extremely high breakdown voltage [26], [105] or entire shielding of dielectric sidewalls [95]. 3D quadrupole traps have also been fabricated using novel techniques which allow for large ion-electrode distances (hence low motional heating rate) for a lower trap drive voltage than surface ion traps [29], [106]. Eltony *et al.* [107] used a transparent material, indium tin oxide (ITO), as the electrode layer to detect fluorescence emitted from ions with a photodetector underneath the electrode on the backside of the trap chip. A selection of various microfabricated ion traps, which includes both surface and 3D quadrupole traps, are shown in Figure 3.2.

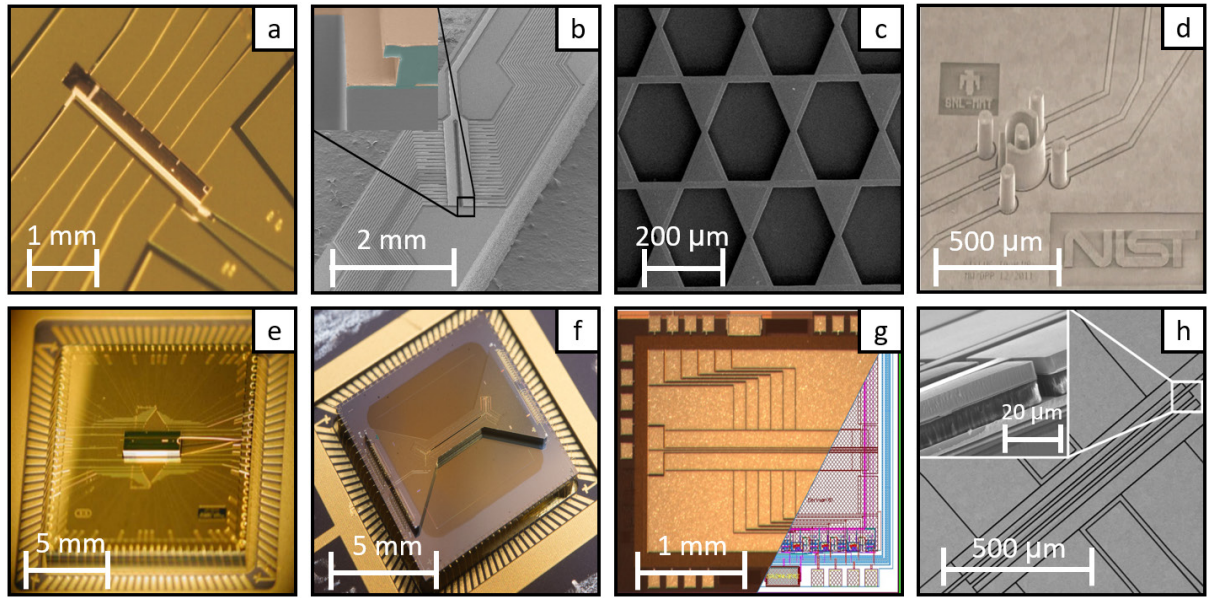


Figure 3.2 – Images of reported ion traps **(a)** Microfabricated, 3D quadrupole trap - National Physics Laboratory (NPL) - Wilpers *et al.* [29] **(b)** Low dielectric exposure - Seoul National University – Hong *et al.* [95] **(c)** First 2-D array on a chip and high breakdown voltage - University of Sussex – Sterling *et al.* [26] **(d)** Large metal structures – National Institute of Standards and Technology (NIST) – Arrington *et al.* [108] **(e)** Through Silicon Via (TSV) in an ion trap - GTRI/Honeywell – Guise *et al.* [102] **(f)** High optical access – Sandia National Laboratory (SNL) – Moehring *et al.*/ Maunz [51], [55] **(g)** Ion trap fabricated in a CMOS foundry - Massachusetts Institute of Technology (MIT) – Stuart *et al.* [32] **(h)** Novel fabrication method for thick metal/dielectric layers - Physikalisch-Technische Bundesanstalt (PTB) – Bautista-Salvador *et al.* [103].

In order to integrate various on-chip features, post or pre-processing steps can be added to the fabrication flow of the basic ion trap structures described previously. As an example of post processing, a vertical slot penetrating the silicon substrate can be fabricated using a conventional deep silicon etching process at the end of ion trap fabrication. This hole can be used to load neutral atoms [109] or to provide increased optical access [110]. For the integration of optical or electrical devices, discussed further in Section 4, the ion trap is fabricated on top of pre-processed wafers where the integrated feature has already been fabricated. This inevitably introduces restrictions on the processes and materials used, hence these concerns should be addressed to provide cross-compatibility between fabrications. For ion traps which use multiple integrated technologies, compatibility between processes can be an exponentially difficult problem to solve and will likely become a strong focus of the community.

BOX 3: Efforts to deal with heating rates

Despite many successful implementations of surface traps, miniaturising the ion trap structure has also created a number of side effects, and one of the drawbacks is the so-called “anomalous heating” of trapped ions [21]. This is thought to be induced by electric field noise from the surface of trap electrodes. The electric field noise can couple to the ion motion when the frequency is near the motional frequency of the ion, which in turn leads to the increase of phonon number to the detriment of quantum systems. Many efforts have been made to investigate this both theoretically [111], [112] and experimentally [113]–[115]. One method of reducing the heating rate is by increasing the distance, d , between the ions and the electrode surface, since it has been experimentally shown that the heating rate scales as $\sim d^{-4}$ [114], [116], [117]. However, given that the maximum voltage that can be applied to a trap chip is limited by current semiconductor technologies, an increased distance inevitably leads to a shallower trap depth, therefore there is a limit to how much d can be increased by. Another method to reduce the heating rate is by cooling the ion trap to cryogenic temperature, first demonstrated in [114]. A number of publications showed that this approach can reduce the heating rate by two orders of magnitude [61], [114], [118]. Other approaches use in-situ cleaning of the chip surface [96], [119]. Since hydrocarbon-based contaminants adsorbed on the electrode surface during the bake-out process are suspected to be a major source of the electrical noise, inducing anomalous heating [120], removal of the contaminants after the bake-out can also reduce the heating rate by two orders of magnitude. Owing to these efforts, extremely low heating rates of ions have been reported [100]. More work is required and is currently under way to better understand the source of anomalous heating [121]–[126]. A current summary of heating rates in microfabricated ion traps as a function of ion-electrode distance is shown Figure 3.3.

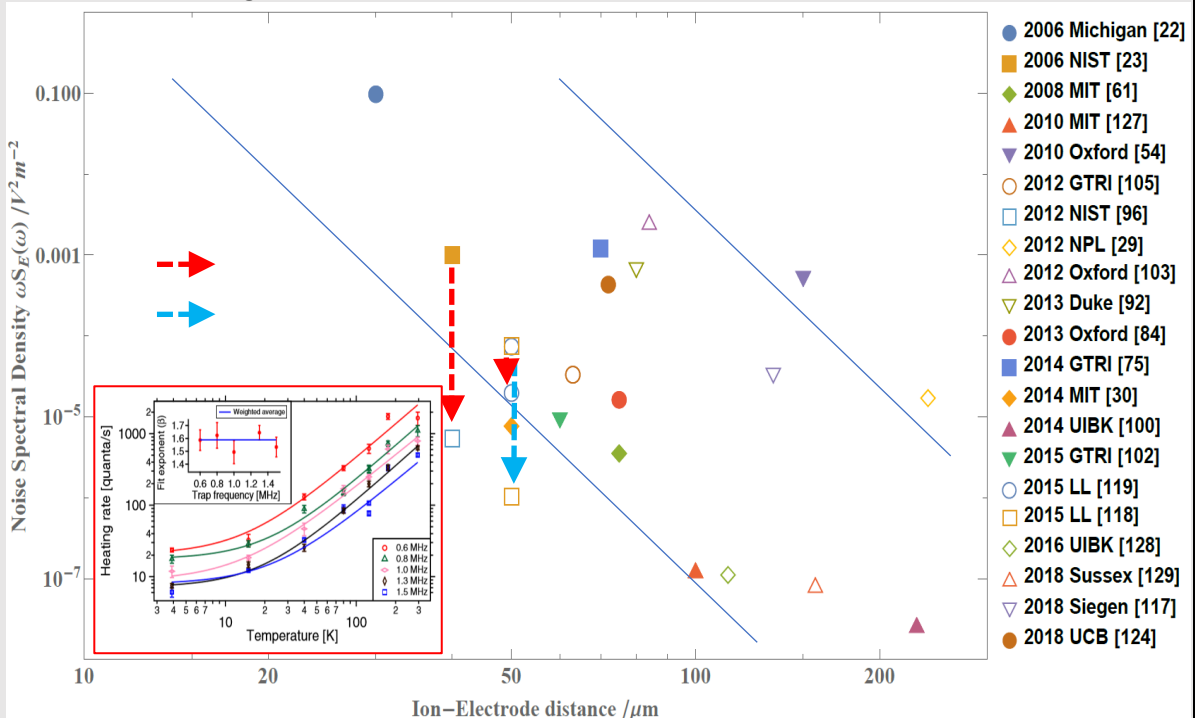


Figure 3.3. Measurement results of heating rates, expressed as noise spectral density, on surface ion traps from different research groups. The heating rates measured in a cryogenic environment (yellow, hollow square) are noticeably lower than that of room temperature systems. The red and blue arrows indicate the changes made in the same experimental setup by in-situ surface cleaning and cryogenic cooling, respectively. The inset (taken from Bruzewicz *et al.* [118]) shows the temperature dependency on heating rate, showing significant gains from room temperature to cryogenic temperatures.

4. Advanced On-Chip Features

As ion trap geometries become more complex, either for quantum simulation or scalable computation purposes, supporting systems are often required to sit within the footprint of the ion trap device [19]. Such efforts include integrating optical and electrical devices used in experiments, into the microchip. These approaches can also contribute to the miniaturisation of precise measurement units such as atomic clocks and mass spectrometers, combined with efforts to miniaturise vacuum chambers [24], [34].

This section will mainly discuss research into chip-level integration of advanced features. Several of the processes for advance feature integration use fabrication methods or materials not described in this manuscript.

4.1 Embedded Gate Schemes

Several schemes for quantum logic gates between qubits rely on magnetic field gradients, either static [130], [131] or oscillating [132], [133]. Three methods to create the gradient have been used: permanent magnets, placed near the trap to produce a static gradient at the ion position [131], [134]–[136]; in-plane current carrying wires (CCWs), fabricated as part of the electrode layer, which allow the creation of both static and oscillating magnetic field gradients [84], [137]–[139]; sub-surface current carrying wires, fabricated below the electrode and ground plane layers [140].

Permanent magnets are commonly implemented to realise the static gradient scheme, achieving gradients of up to 36 T m^{-1} [136]. Scaling up to large systems may prove difficult due to careful, manual alignment of the ion trap to the magnets being required.

In-plane CCWs have been shown to provide oscillating gradients of up to 54.8 T m^{-1} [85]. In this scheme the trap geometry must be altered in order to accommodate the CCWs and the power dissipation must be considered. The power dissipation could be reduced by using thicker layers, to decrease resistance, however the skin depth of the oscillating field in the electrodes may quickly limit this, depending on the transition required and electrode material.

Sub-surface CCWs, situated beneath the ion trap, do not impinge on the electrode design and can be used for both static and oscillating gradients. For the latter, the field is likely to be attenuated due to shielding by induced currents in the ion trap electrodes and ground plane layers. The device of Welzel *et al.* [140], used Cu wires $127 \mu\text{m}$ thick, fixed to an AlN chip carrier and mounted $285 \mu\text{m}$ below the trap surface. A gradient of 16 T m^{-1} was achieved using a current of 8.4 A .

Larger gradients could be achieved with sub-surface CCWs by reducing the wire to ion distance. Lekitsch *et al.* [19] suggest that the CCWs could be imbedded into the substrate surface, using the dual damascene process, and the ion trap fabricated directly above the wires. By embedding the CCWs into the substrate, not only is the trap to wire distance decreased, but thermal sinking is improved, thus greater current, and therefore higher gradients, should be feasible [19]. At the University of Sussex, we have already demonstrated applying a current of 11 A (corresponding to a current density of 10^6 A cm^{-2}) to an ion microchip which should result in a magnetic field gradient of $>185 \text{ T m}^{-1}$ at an ion height of $125 \mu\text{m}$. At an ion height of $40 \mu\text{m}$, this method is expected to produce a gradient in excess of $1,000 \text{ T m}^{-1}$ or conversely obtain $\sim 185 \text{ T m}^{-1}$ with significantly lower current required ($\sim 3 \text{ A}$).

Whilst a relatively new technology for ion traps, CCWs are common place in the atom-trapping community, where large, steep magnetic fields are used to trap neutral systems [141]–[144]. The currents and wire dimensions used for atom trapping are similar to those required by trapped ion gate

schemes and therefore much of what has been learned in the atom trapping field may also be applicable.

4.2 Optical Components

For many trapped ion technologies addressing and state readout of ions is required using optical techniques on an individual ion basis. It is sometimes beneficial that such optical components are integrated in the device, to increase the fidelity of addressing and readout operations. This subsection will look at several integrated optical components and examine their uses.

Optical fibres have many uses in trapped ion experiments for both addressing and readout operations. The typical structure of a fibre however does not naturally suit itself to an ion trapping experiment as an exposed dielectric near the ion can significantly disturb the trapping field. By integrating an optical access hole, the dielectric can be shielded by the ion trap itself, allowing for fibres to be brought close to the ion [82], [110], [145].

To address multiple ions, integrating waveguides into the ion trap is a promising way forward. Mehta *et al.* [146], [147] demonstrated a multi-ion addressing technique with integrated silicon nitride waveguides and grating couplers to address individual ions, with a total optical system loss of 33dB. Using integrated waveguides, Niffenegger *et al.* [148] have recently delivered multiple wavelengths of light to a trapped ion. This demonstration has been combined with packaging methods which allow for a direct optical fibre attach to the waveguides. Using this, a single qubit gate with $^{88}\text{Sr}^+$ was performed with 99% fidelity [147] and two qubit gates have also been recently demonstrated [149]. Another approach for the scalable laser addressing is adjusting beam paths with electrically controlled devices. Crain *et al.* [150], demonstrated controlled beam steering with MEMS mirrors, however such technology has yet to be integrated into a trap.

Integrating mirrors into the ion trap surface can allow for more photons from the ion to be collected, by reflecting otherwise lost photons. Merrill *et al.* [151] integrated micro mirrors into their surface ion trap, enhancing photon collection of $^{40}\text{Ca}^+$ by 90% which resulted in a collection efficiency of 14% (numerical aperture of 0.69). Ghadmi *et al.* [152] showed a 4.1(6) % coupling of the fluorescence from a $^{174}\text{Yb}^+$ ion into a single mode fibre using integrated diffractive mirrors, which nearly tripled the bulk optics efficiency. Integrated mirrors can also be used to create cavities on chip to, for instance, facilitate atom-light coupling for photonic interconnects. Towards this endeavour, ion traps fabricated on top of high-finesse optical mirrors to create a cavity have been demonstrated [153], [154]. There remains, however, some development before strong coupling, already demonstrated macroscopically [155], can be achieved in such a microfabricated device.

Standard ion trapping detection uses large collection optics which helps counteract the effect of being outside the vacuum system and hence further from the ion [156]. By integrating a detector into the actual trap chip, the detector-ion distance decreases which could help capturing more photons with appropriate optics in place. Kielpinski *et al.* [157] and Lekitsch *et al.* [19] suggested using integrated single photon avalanche diodes (SPADs) for light detection. Eltony *et al.* [107] presented a transparent trap made of ITO with an integrated photodetector featuring a collection efficiency approaching 50%. Slichter *et al.* [31] showed UV-sensitive superconducting nanowire single photon detectors (SNSPD) made of MoSi, integrated into a microfabricated ion trap. This device demonstrated a detector fidelity of 76(4) % at a wavelength of 315nm with a background count rate below 1 count per second. The trapping field decreased the system detection efficiency by 9%, but did not increase background count rates. Being a superconducting device however, the stringent requirement on the operating temperature (3.2 K) introduces additional challenges, depending on the application. The use of SPADs

however only requires temperatures of 70K in order to achieve a performance similar to a photomultiplier tube [19].

4.3 Passive Components

Capacitors, resistors and inductors are a key part of any ion trapping experiment for use in filtering, resonators and general electronics [24], [104], [158], [159]. Bringing these devices on-chip can have a multitude of benefits, from increased density to reduced noise via closer proximity to the device.

One method of high-density integration of passive components takes advantage of advanced CMOS facilities by integrating a CMOS die. Guise *et al.* [33] first showed this by integrating a Semiconwell SWTF¹ 12 channel, bare-die RC filter array (35kΩ, 220pF) on to a PCB. To attach the die, a standard low-outgassing silver epoxy was used, and channels were connected using wirebonds. Whilst not integrated on chip, the attach methods are similar to that used by industry on silicon dies, hence could be integrated on an ion trap if required. Using methods afforded by modern CMOS facilities [32] and careful calibration, one could feasibly fabricate resistive temperature probes in the trap. Conversely, a resistive strip could also act as a local heater for use in cryogenic systems to prevent gas molecules freezing out on the trap during preparation [100].

Capacitors can be fabricated into the trap with two metal planes separated by a dielectric. Trench capacitors take advantage of increased surface area by etching vertically into silicon using well established processes. This allows for a substantial increase in the capacitance per unit area. For ion traps, this was first demonstrated by Allcock *et al.* [104], who integrated trench capacitors into their trap, which allowed 1nF to be achieved in a 100μm square. This was 30 times higher than the capacitance allowed in the same area when using a conventional, planar, fabrication process. A capacitive divider is a common method for one to measure the large RF voltage applied to the ion trap [160]. Such a component could be integrated into the device itself using the methods discussed previously.

To create the low-noise, high voltage RF trapping field, a helical resonator is commonly employed [161], [162]. At the heart of the design is the ability to impedance match using inductors. Efforts have been made to reduce the bulky nature of the device to a more manageable size [163], [164], but have yet to be integrated into a device. Microfabricated inductors [165] could be one route forward in this respect. For future devices, microfabricated inductors could also be used to replace the standard low-pass filter [104] with more advanced filters, such as a band-stop filter, to remove noise on DC electrodes.

4.4 Active Components

Rent's Rule [166] suggests that computers were only successful by changing the scaling law on the number of inputs required to control bits. The same thinking has also been suggested for quantum computation [167]. These connectivity problems naturally lead to the introduction of active components into the vacuum system [33], or even into the ion trap [32]. One of the key requirements for ion-trapping is that all integrated components must be UHV compatible [168]. This often eliminates the use of packaged electronics, making bare-die an alternative for inclusion in a UHV environment. Packaged components can sometimes be permitted if also operating at cryogenic temperatures. Guise *et al.* [33] introduced two, 40 channel DACs (AD5370) into an UHV environment. For this experiment, the AD5370 was not sourced in bare-die form, but instead a standard, packaged, AD5370 was used and then decapsulated using nitric and sulphuric acid [169]. Assembly is as discussed in Section 4.3. Whilst this is a novel method to overcome low supply of bare-die products, it is likely

¹ http://www.semiconwell.com/rc_net/swtf.htm

that future devices using this method would already be in bare-die form, hence suitable for ultra-high vacuum.

Stuart *et al.* [32] recently integrated a custom, CMOS DAC into an ion trap. The custom DAC was designed for the CMHV7SF 180nm node from Global Foundries. Key to this node is the ability to allow for higher voltages (20V span) compared to typical <5V span, thus allowing the implementation of an amplifier for voltages more suited for ion trapping. A switching device was also included to disconnect the ion trap from the DAC when not updating, hence reducing noise when disconnected. As the electrode acts as a capacitor with low leakage current, the switch can disconnect the DAC whilst the electrode holds a voltage. The ion trap on top was also fabricated as part of the CMOS process, similar to that used by Mehta *et al.* [30]. A common concern with semiconductor devices is ‘freeze-out’ at low temperatures, where the energy required to overcome a band-gap is insurmountable. However the device previously mentioned was operated at cryogenic (4K) temperatures and more complicated devices such as a field programmable gate array (FPGA) have also been shown to work at such temperatures [170].

4.5 Stacked Wafer Technology

It has been proposed that back-side connections to the ion trap will be required for a large-scale quantum computer to connect to its supporting systems [102]. Lekitsch *et al.* [19] expand this to use wafer stacking of different components of the quantum computing stack, such as DACs, detectors, and cooling. These proposals require the introduction of through-substrate-via technology, often known as through-silicon-vias (TSV). The first demonstration of these technologies in ion traps was reported by Guise *et al.* [102], who connected an ion trap via a backside ball-grid array and TSVs. In [102], the ion trap die is attached via a ball-bonding method, which uses a programmed gold ball bonder to leave individual short, gold studs on an interposer. A localised eutectic bond is then used to connect the interposer to the back-side of the device. For a wafer-scale bonding, issues occur with high stress (due to device size), reducing connection quality [171]. On a wafer-scale, the studs are commonly microfabricated as opposed to using a ball bonder [172]. Eutectic bonding is also not the only option for wafer-scale attaches and many other, commonly used, methods exist [173], [174].

Lekitsch *et al.* [19] suggest the implementation of micro-channel cooling as part of the stacked wafer proposal. This could also be used in other architectures, either for power dissipation or to reduce heating rates. Whilst they have yet to be introduced into ion traps, micro-channel coolers have started to emerge for room temperature devices capable of removing $>300\text{W/cm}^2$ [175]. Riddle and Bernhardt [176] demonstrated a micro-channel cooler using liquid nitrogen capable of removing 1000W/cm^2 , considerably helped by an order-of-magnitude increase in thermal conductivity of Silicon at $\sim 70\text{K}$ [177]. Difficulties with this design however may emerge from heat-flow between stacked wafer levels and work is still required to develop heat-flow mechanisms between wafers.

5. Conclusion

Much progress has been made in recent years on the development of complex microfabricated ion traps. Whilst the creation of custom potentials through simulations is well understood, many questions still must be answered in terms of the integration of advanced technologies. We present Figure 5.1 as a summary of the requirements for many different advanced ion traps. With most of these technologies having already been individually demonstrated in trapped ion experiments, the microfabricated ion trap is expected to form a fundamental component of quantum technologies.

5.1 Outlook

Demand for quantum technologies, as a commercial product, requires that devices can be made on a large scale, with high reliability and yields. The following section will discuss the current state of these technologies.

Many of the proposed technologies discussed will require CMOS devices integrated into the ion trap. However, unlike the standard operation environment of CMOS, ion traps are often required to work at cryogenic temperatures. Interestingly, cryogenic control electronics is also a priority for superconducting qubit platforms [178] and solid-state qubits [179]. Cryogenic CMOS integration of a DAC has recently been demonstrated by Stuart *et al.* [32] which already has the capability to be mass produced. Whilst commercialised SNSPDs are relatively uncommon, SPADs are becoming increasingly wide-spread, with high demand from the driverless car market. SNSPDs may prove simpler to integrate as they can be fabricated as part of the ion trap, however, they have to be operated at superconducting temperatures. Waveguide-on-chip technology is a developing field with many applications across the spectrum of quantum technologies. As a result, several fabrication facilities have appeared in recent years which can offer some of the commercial capabilities required for the optical components discussed. Further development however is still needed in this field to create optical components with greater suitability for blue and near UV wavelengths as well as introducing such components to an industrial scale process. Wafer stacking and TSVs, whilst nascent technologies, are becoming prevalent in many different modern devices, such as high-bandwidth memory [180], and is a well-understood process [181]. Cooling requirements will become increasingly important to consider when integrating different technologies. Microchannel coolers provide a promising path towards managing the potential future thermal requirements however they have yet to reach market.

Whilst fabrication and assembly industries allow individual aspects of an ion trap to be demonstrated, combining these technologies will be essential for creating a more advanced ion trap. Separating the technologies on a wafer-by-wafer level may prove prudent in reducing risks of compatibility but introduces new issues with inter-wafer connectivity for large devices and heat flow. Whilst integrating electronics can reduce some noise by closer proximity of supporting electronics and therefore less ‘pick-up’, it can introduce new noise spectrums due to the integration of active components. This can be mitigated through additional filtering as well as noise manipulation to move the noise spectrum to frequencies that do not affect the ion. Some of the optical technologies discussed will perform optimally only at certain wavelengths. Integrating many of these optical components could therefore require multi-species schemes to best take advantage of these technologies [182]–[186]. With a large variety of technologies being simultaneously integrated, unforeseen consequences will be a likely occurrence, hence full integration will remain a tremendous engineering challenge.

5.2 Concluding Remarks

In this paper we have motivated modern design choices in ion traps and highlighted their relevance to modern experiments. We have covered the basics of ion trapping and how ion traps fit into a typical experiment. We discussed how ion trap geometries are determined and how they are adapted to novel designs for different applications. We presented a typical fabrication flow for a modern device by looking at current state-of-the-art fabrications, as well as efforts to tackle heating rates. We examined advanced on-chip features such as optical components, electronics, and methods to integrate this into modular structures. Finally, we highlighted what the authors believe to be the current struggles in microfabricated ion traps and how these conform to modern industrial capabilities.

Trapped ions constitute an extremely powerful system to realise and control quantum phenomena such as entanglement and superposition, showcasing unmatched fidelities and coherence times. The emergence of ion microchips allows us to incorporate the advantages of modern microfabrication and microprocessor advances to this system, giving rise to a fully scalable hardware platform for a wide range of quantum technologies.

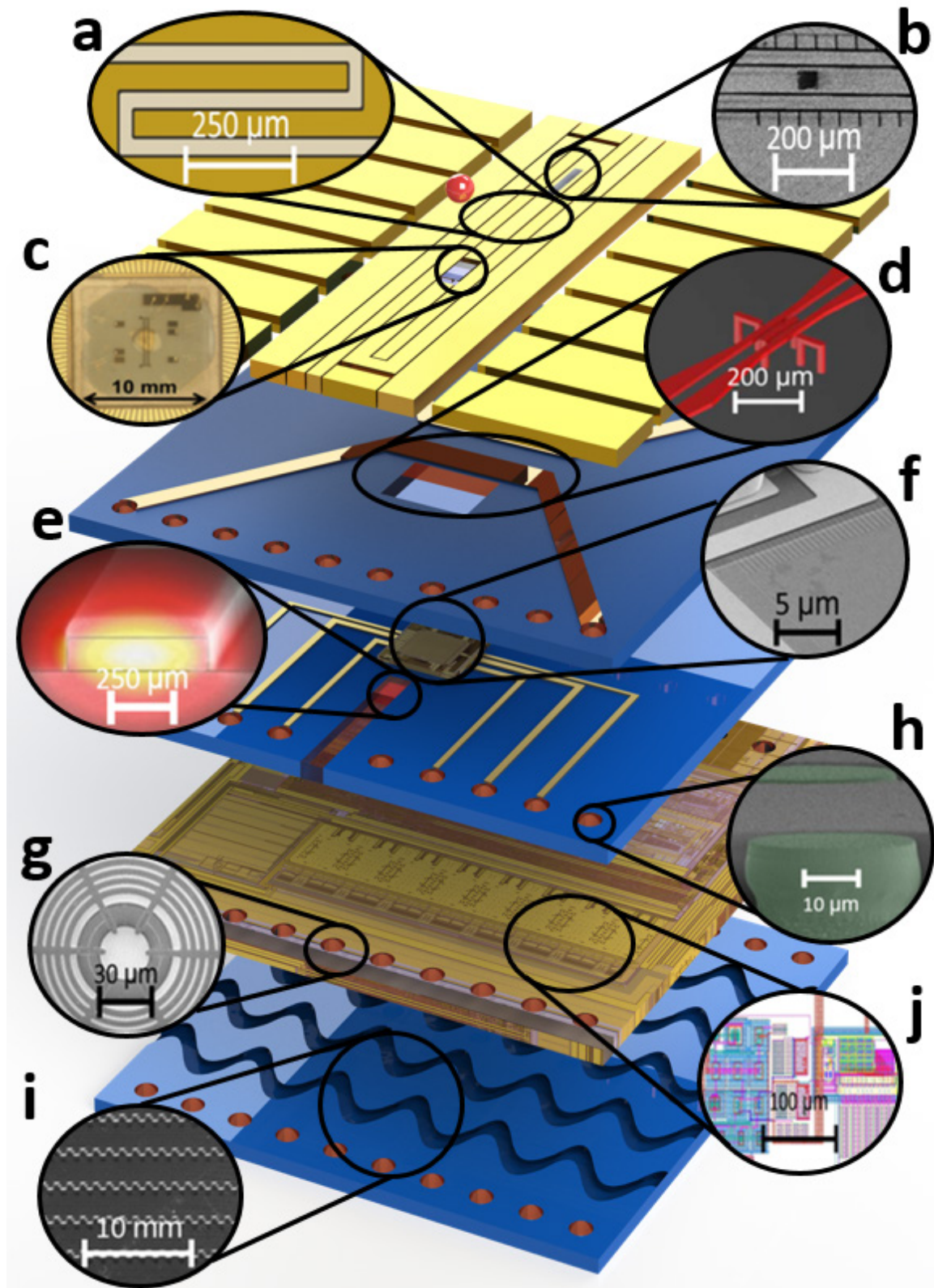


Figure 5.1 – Advanced on chip technology in an ion trap. It should be noted that not all features are required and their necessity is dependent upon use case. **(a)** Oscillating gradient CCWs [138] **(b)** Backside loading [76] **(c)** Transparent ITO electrode [107] **(d)** Static gradient CCWs [19] **(e)** Si_3N_4 waveguide and grating for individual optical addressing [147] **(f)** Integrated photon detector [31] **(g)** Trench capacitors [102] **(h)** Through Silicon Vias (TSVs) [102] **(i)** Microchannel cooling [175] **(j)** Integrated electronics [32].

6. Acknowledgements

This work is supported by the U.K. Engineering and Physical Sciences Research Council via the EPSRC Hub in Quantum Computing and Simulation (EP/T001062/1), the U.K. Quantum Technology hub for Networked Quantum Information Technologies (No. EP/M013243/1), the European Commission’s Horizon-2020 Flagship on Quantum Technologies Project No. 820314 (MicroQC), the U.S. Army Research Office under Contract No. W911NF-14-2-0106, the Fonds National de la Recherche Luxembourg (National Research Fund) Project Code 11615035 and the University of Sussex.

7. References

- [1] W. Paul, “Electromagnetic traps for charged and neutral particles,” *Rev. Mod. Phys.*, vol. 62, no. 3, pp. 531–540, Jul. 1990.
- [2] H. Dehmelt, “Experiments with an Isolated Subatomic Particle at Rest (Nobel Lecture),” *Angew. Chemie Int. Ed. English*, vol. 29, no. 7, pp. 734–738, 1990.
- [3] D. J. Wineland and W. M. Itano, “Laser cooling of atoms,” *Phys. Rev. A*, vol. 20, no. 4, pp. 1521–1540, 1979.
- [4] J. J. Bollinger, D. J. Heizen, W. M. Itano, S. L. Gilbert, and D. J. Wineland, “A 303-MHz frequency standard based on trapped Be^{+} ions,” *IEEE Trans. Instrum. Meas.*, vol. 40, no. 2, pp. 126–128, Apr. 1991.
- [5] Y. Wang *et al.*, “Single-qubit quantum memory exceeding ten-minute coherence time,” *Nat. Photonics*, vol. 11, no. 10, pp. 646–650, Oct. 2017.
- [6] A. D. Ludlow, M. M. Boyd, J. Ye, E. Peik, and P. O. Schmidt, “Optical atomic clocks,” *Rev. Mod. Phys.*, vol. 87, no. 2, pp. 637–701, Jun. 2015.
- [7] I. Baumgart, J.-M. Cai, A. Retzker, M. B. Plenio, and C. Wunderlich, “Ultrasensitive Magnetometer using a Single Atom,” *Phys. Rev. Lett.*, vol. 116, no. 24, p. 240801, Jun. 2016.
- [8] D. Porras and J. I. Cirac, “Effective Quantum Spin Systems with Trapped Ions,” *Phys. Rev. Lett.*, vol. 92, no. 20, p. 207901, 2004.
- [9] R. Blatt and C. F. Roos, “Quantum simulations with trapped ions,” *Nat. Phys.*, vol. 8, no. 4, pp. 277–284, 2012.
- [10] C. Schneider, D. Porras, and T. Schaetz, “Experimental quantum simulations of many-body physics with trapped ions,” *Reports Prog. Phys.*, vol. 75, no. 2, 2012.
- [11] J. G. Bohnet *et al.*, “Quantum spin dynamics and entanglement generation with hundreds of trapped ions,” *Science (80-)*, vol. 352, no. 6291, pp. 1297–1301, Jun. 2016.
- [12] P. H. Dawson, *Quadrupole Mass Spectrometry and Its Applications*, 1st ed. Elsevier, 1976.
- [13] M. G. Blain *et al.*, “Towards the hand-held mass spectrometer: Design considerations, simulation, and fabrication of micrometer-scaled cylindrical ion traps,” *Int. J. Mass Spectrom.*,

vol. 236, no. 1–3, pp. 91–104, 2004.

- [14] S. Pau *et al.*, “Microfabricated quadrupole ion trap for mass spectrometer applications,” *Phys. Rev. Lett.*, vol. 96, no. 12, pp. 2–5, 2006.
- [15] J. I. I. Cirac and P. Zoller, “Quantum Computations with Cold Trapped Ions,” *Phys. Rev. Lett.*, vol. 74, no. 20, pp. 4091–4094, May 1995.
- [16] A. Bermudez *et al.*, “Assessing the progress of trapped-ion processors towards fault-tolerant quantum computation,” *Phys. Rev. X*, vol. 7, no. 4, pp. 1–41, 2017.
- [17] D. Kielpinski, C. Monroe, and D. J. Wineland, “Architecture for a large-scale ion-trap quantum computer,” *Nature*, vol. 417, no. 6890, pp. 709–711, Jun. 2002.
- [18] C. Monroe and J. Kim, “Scaling the Ion Trap Quantum Processor,” *Science (80-.)*, vol. 339, no. 6124, pp. 1164–1169, Mar. 2013.
- [19] B. Lekitsch *et al.*, “Blueprint for a microwave trapped ion quantum computer,” *Sci. Adv.*, vol. 3, no. 2, p. e1601540, Feb. 2017.
- [20] M. A. Rowe *et al.*, “Transport of Quantum States and Separation of Ions in a Dual RF Ion Trap,” *Quantum Inf. Comput.*, vol. 1, no. 0, p. 15, May 2002.
- [21] Q. A. Turchette *et al.*, “Heating of trapped ions from the quantum ground state,” *Phys. Rev. A - At. Mol. Opt. Phys.*, vol. 61, no. 6, p. 8, 2000.
- [22] D. Stick, W. K. Hensinger, S. Olmschenk, M. J. Madsen, K. Schwab, and C. Monroe, “Ion trap in a semiconductor chip,” *Nat. Phys.*, vol. 2, no. 1, pp. 36–39, 2006.
- [23] S. Seidelin *et al.*, “Microfabricated surface-electrode ion trap for scalable quantum information processing,” *Phys. Rev. Lett.*, vol. 96, no. 25, pp. 1–5, 2006.
- [24] G. Wilpers, P. See, P. Gill, and A. G. Sinclair, “A compact UHV package for microfabricated ion-trap arrays with direct electronic air-side access,” *Appl. Phys. B Lasers Opt.*, vol. 111, no. 1, pp. 21–28, 2013.
- [25] P. D. D. Schwindt *et al.*, “A highly miniaturized vacuum package for a trapped ion atomic clock,” *Rev. Sci. Instrum.*, vol. 87, no. 5, p. 053112, 2016.
- [26] R. C. Sterling *et al.*, “Fabrication and operation of a two-dimensional ion-trap lattice on a high-voltage microchip,” *Nat. Commun.*, vol. 5, p. 3637, 2014.
- [27] M. Mielenz *et al.*, “Arrays of individually controlled ions suitable for two-dimensional quantum simulations,” *Nat. Commun.*, vol. 7, no. May, pp. 1–9, 2016.
- [28] J. Chiaverini *et al.*, “Surface-Electrode Architecture for Ion-Trap Quantum Information Processing,” *Quantum Info Comput.*, vol. 5, pp. 419–439, Jan. 2005.
- [29] G. Wilpers, P. See, P. Gill, and A. G. Sinclair, “A monolithic array of three-dimensional ion traps fabricated with conventional semiconductor technology,” *Nat. Nanotechnol.*, vol. 7, no. 9, pp. 572–576, Jul. 2012.
- [30] K. K. Mehta *et al.*, “Ion traps fabricated in a CMOS foundry,” *Appl. Phys. Lett.*, vol. 105, no. 4, p. 044103, Jul. 2014.
- [31] D. H. Slichter, V. B. Verma, D. Leibfried, R. P. Mirin, S. W. Nam, and D. J. Wineland, “UV-sensitive superconducting nanowire single photon detectors for integration in an ion trap,” *Opt. Express*, vol. 25, no. 8, p. 8705, Apr. 2017.

- [32] J. Stuart *et al.*, “Chip-Integrated Voltage Sources for Control of Trapped Ions,” *Phys. Rev. Appl.*, vol. 11, no. 2, p. 024010, Feb. 2019.
- [33] N. D. Guise *et al.*, “In-Vacuum Active Electronics for Microfabricated Ion Traps,” *Rev. Sci. Instrum.*, vol. 85, no. May 2015, p. 063101, 2014.
- [34] K. R. Brown, J. Kim, and C. Monroe, “Co-designing a scalable quantum computer with trapped atomic ions,” *npj Quantum Inf.*, vol. 2, no. August, p. 16034, 2016.
- [35] M. D. Hughes, B. Lekitsch, J. A. Broersma, and W. K. Hensinger, “Microfabricated ion traps,” *Contemp. Phys.*, vol. 52, no. 6, pp. 505–529, Nov. 2011.
- [36] J. M. Amini, J. Britton, D. Leibfried, and D. J. Wineland, “Micro-Fabricated Chip Traps for Ions,” *Atom Chips*, pp. 395–420, 2011.
- [37] E. Mount *et al.*, “Scalable digital hardware for a trapped ion quantum computer,” *Quantum Inf. Process.*, vol. 15, no. 12, pp. 5281–5298, Dec. 2016.
- [38] D. I. “Dan” Cho, S. Hong, M. Lee, and T. Kim, “A review of silicon microfabricated ion traps for quantum information processing,” *Micro Nano Syst. Lett.*, vol. 3, no. 1, pp. 31–34, 2015.
- [39] A. M. Eltony, D. Gangloff, M. Shi, A. Bylinskii, V. Vuletić, and I. L. Chuang, “Technologies for trapped-ion quantum information systems,” *Quantum Inf. Process.*, vol. 15, no. 12, pp. 5351–5383, Dec. 2016.
- [40] C. D. Bruzewicz, J. Chiaverini, R. McConnell, and J. M. Sage, “Trapped-ion quantum computing: Progress and challenges,” *Appl. Phys. Rev.*, vol. 6, no. 2, p. 021314, Jun. 2019.
- [41] W. Neuhauser, M. Hohenstatt, P. E. Toschek, and H. Dehmelt, “Localized visible Ba⁺ mono-ion oscillator,” *Phys. Rev. A*, vol. 22, no. 3, pp. 1137–1140, 1980.
- [42] C. Monroe, D. M. Meekhof, B. E. King, W. M. Itano, and D. J. Wineland, “Demonstration of a fundamental quantum logic gate,” *Phys. Rev. Lett.*, vol. 75, no. 25, pp. 4714–4717, 1995.
- [43] J. D. Prestage, G. J. Dick, and L. Maleki, “New ion trap for frequency standard applications,” *J. Appl. Phys.*, vol. 66, no. 3, pp. 1013–1017, 1989.
- [44] M. G. Raizen, J. M. Gilligan, J. C. Bergquist, W. M. Itano, and D. J. Wineland, “Ionic crystals in a linear Paul trap,” *Phys. Rev. A*, vol. 45, no. 9, pp. 6493–6501, May 1992.
- [45] D. J. Berkeland, J. D. Miller, J. C. Bergquist, W. M. Itano, and D. J. Wineland, “Minimization of ion micromotion in a Paul trap,” *J. Appl. Phys.*, vol. 83, no. 10, pp. 5025–5033, 1998.
- [46] F. Schmidt-Kaler *et al.*, “Realization of the Cirac–Zoller controlled-NOT quantum gate,” *Nature*, vol. 422, no. 6930, pp. 408–411, Mar. 2003.
- [47] T. Monz *et al.*, “14-qubit entanglement: Creation and coherence,” *Phys. Rev. Lett.*, vol. 106, no. 13, pp. 1–4, 2011.
- [48] S. Debnath, N. M. Linke, C. Figgatt, K. A. Landsman, K. Wright, and C. Monroe, “Demonstration of a small programmable quantum computer with atomic qubits,” *Nature*, vol. 536, no. 7614, pp. 63–66, 2016.
- [49] N. Friis *et al.*, “Observation of Entangled States of a Fully Controlled 20-Qubit System,” *Phys. Rev. X*, vol. 8, no. 2, p. 021012, Apr. 2018.
- [50] M. J. Madsen, W. K. Hensinger, D. Stick, J. a. Rabchuk, and C. Monroe, “Planar ion trap geometry for microfabrication,” *Appl. Phys. B Lasers Opt.*, vol. 78, no. 5, pp. 639–651, 2004.

- [51] D. L. Moehring *et al.*, “Design, fabrication and experimental demonstration of junction surface ion traps,” *New J. Phys.*, vol. 13, 2011.
- [52] D. J. Wineland, C. Monroe, W. M. Itano, D. Leibfried, B. E. King, and D. M. Meekhof, “Experimental Issues in Coherent Quantum-State Manipulation of Trapped Atomic Ions,” *J. Res. Natl. Inst. Stand. Technol. [J. Res. Natl. Inst. Stand. Technol.]*, vol. 103, no. 103, pp. 1689–1699, 1998.
- [53] J. I. Cirac and P. Zoller, “A scalable quantum computer with ions in an array of microtraps,” *Nature*, vol. 404, no. 6778, pp. 579–581, Apr. 2000.
- [54] D. T. C. Allcock *et al.*, “Implementation of a symmetric surface-electrode ion trap with field compensation using a modulated Raman effect,” *New J. Phys.*, vol. 12, 2010.
- [55] P. L. W. Maunz, “High Optical Access Trap 2.0.,” https://prod.sandia.gov/sand_doc/2016/160796r.pdf. Sandia National Laboratories, Albuquerque, NM, and Livermore, CA (United States), 26-Jan-2016.
- [56] M. G. House, “Analytic model for electrostatic fields in surface-electrode ion traps,” *Phys. Rev. A - At. Mol. Opt. Phys.*, vol. 78, no. 3, pp. 1–8, 2008.
- [57] J. H. Wesenberg, “Electrostatics of surface-electrode ion traps,” *Phys. Rev. A*, vol. 78, no. 6, p. 063410, 2008.
- [58] R. Schmied, “Electrostatics of gapped and finite surface electrodes,” *New J. Phys.*, vol. 12, 2010.
- [59] C. E. Pearson, D. R. Leibrandt, W. S. Bakr, W. J. Mallard, K. R. Brown, and I. L. Chuang, “Experimental investigation of planar ion traps,” *Phys. Rev. A*, vol. 73, no. 3, p. 032307, Nov. 2005.
- [60] A. H. Nizamani and W. K. Hensinger, “Optimum electrode configurations for fast ion separation in microfabricated surface ion traps,” *Appl. Phys. B*, vol. 106, no. 2, pp. 327–338, Feb. 2012.
- [61] J. Labaziewicz, Y. Ge, P. Antohi, D. Leibrandt, K. R. Brown, and I. L. Chuang, “Suppression of heating rates in cryogenic surface-electrode ion traps,” *Phys. Rev. Lett.*, vol. 100, no. 1, pp. 1–4, 2008.
- [62] D. Stick *et al.*, “Demonstration of a microfabricated surface electrode ion trap,” *arXiv*, p. 1008.0990v2, Aug. 2010.
- [63] R. Bowler *et al.*, “Coherent diabatic ion transport and separation in a multizone trap array,” *Phys. Rev. Lett.*, vol. 109, no. 8, pp. 1–4, 2012.
- [64] A. Walther *et al.*, “Controlling Fast Transport of Cold Trapped Ions,” *Phys. Rev. Lett.*, vol. 109, no. 8, p. 080501, Aug. 2012.
- [65] H. Kaufmann, T. Ruster, C. T. Schmiegelow, F. Schmidt-Kaler, and U. G. Poschinger, “Dynamics and control of fast ion crystal splitting in segmented Paul traps,” *New J. Phys.*, vol. 16, no. 7, p. 073012, 2014.
- [66] T. Ruster *et al.*, “Experimental realization of fast ion separation in segmented Paul traps,” *Phys. Rev. A*, vol. 90, no. 3, p. 033410, Sep. 2014.
- [67] P. Kaufmann, T. F. Gloge, D. Kaufmann, M. Johanning, and C. Wunderlich, “High-Fidelity Preservation of Quantum Information during Trapped-Ion Transport,” *Phys. Rev. Lett.*, vol. 120, no. 1, p. 010501, Jan. 2018.

- [68] R. Reichle *et al.*, “Transport dynamics of single ions in segmented microstructured Paul trap arrays,” *Fortschritte der Phys.*, vol. 54, no. 8–10, pp. 666–685, 2006.
- [69] D. Hucul, M. Yeo, W. K. Hensinger, J. Rabchuk, S. Olmschenk, and C. Monroe, “On the Transport of Atomic Ions in Linear and Multidimensional Ion Trap Arrays,” *Quantum Inf. Comput.*, vol. 6–7, pp. 501–578, Feb. 2007.
- [70] H. A. Fürst *et al.*, “Controlling the transport of an ion: classical and quantum mechanical solutions,” *New J. Phys.*, vol. 16, no. 7, p. 075007, 2014.
- [71] W. K. Hensinger *et al.*, “T-junction ion trap array for two-dimensional ion shuttling, storage, and manipulation,” *Appl. Phys. Lett.*, vol. 88, no. 3, p. 034101, 2006.
- [72] D. R. Leibrandt *et al.*, “Demonstration of a scalable, multiplexed ion trap for quantum information processing,” *Quantum Inf. Comput.*, vol. 9, no. 11, pp. 901–919, Apr. 2009.
- [73] J. M. Amini *et al.*, “Toward scalable ion traps for quantum information processing,” *New J. Phys.*, vol. 12, 2010.
- [74] R. B. Blakestad *et al.*, “High fidelity transport of trapped-ion qubits through an X-junction trap array,” *Phys. Rev. Lett.*, vol. 102, no. 15, p. 153002, Jan. 2009.
- [75] G. Shu *et al.*, “Heating rates and ion-motion control in a Y-junction surface-electrode trap,” *Phys. Rev. A*, vol. 89, no. 6, p. 062308, Jun. 2014.
- [76] K. Wright *et al.*, “Reliable transport through a microfabricated X-junction surface-electrode ion trap,” *New J. Phys.*, vol. 15, p. 033004, Oct. 2013.
- [77] A. Mokhberi, R. Schmied, and S. Willitsch, “Optimised surface-electrode ion-trap junctions for experiments with cold molecular ions,” *New J. Phys.*, vol. 19, no. 4, 2017.
- [78] R. B. Blakestad *et al.*, “Near-ground-state transport of trapped-ion qubits through a multidimensional array,” *Phys. Rev. A - At. Mol. Opt. Phys.*, vol. 84, no. 3, pp. 1–14, 2011.
- [79] R. Schmied, J. H. Wesenberg, and D. Leibfried, “Optimal surface-electrode trap lattices for quantum simulation with trapped ions,” *Phys. Rev. Lett.*, vol. 102, no. 23, pp. 2–5, 2009.
- [80] F. Hakelberg, P. Kiefer, M. Wittemer, U. Warring, and T. Schaetz, “Interference in a Prototype of a Two-Dimensional Ion Trap Array Quantum Simulator,” *Phys. Rev. Lett.*, vol. 123, no. 10, p. 100504, 2019.
- [81] F. N. Krauth, J. Alonso, and J. P. Home, “Optimal electrode geometries for 2-dimensional ion arrays with bi-layer ion traps,” *J. Phys. B At. Mol. Opt. Phys.*, vol. 48, no. 1, 2015.
- [82] A. P. VanDevender, Y. Colombe, J. Amini, D. Leibfried, and D. J. Wineland, “Efficient fiber optic detection of trapped ion fluorescence,” *Phys. Rev. Lett.*, vol. 105, no. 2, pp. 1–4, 2010.
- [83] K. Singer *et al.*, “Colloquium: Trapped ions as quantum bits -- essential numerical tools,” *Rev. Mod. Phys.*, vol. 82, no. 3, pp. 2609–2632, Dec. 2009.
- [84] D. T. C. Allcock *et al.*, “A microfabricated ion trap with integrated microwave circuitry,” *Appl. Phys. Lett.*, vol. 102, no. 4, 2013.
- [85] H. Hahn *et al.*, “Multilayer ion trap with three-dimensional microwave circuitry for scalable quantum logic applications,” *Appl. Phys. B*, vol. 125, no. 8, p. 154, Aug. 2019.
- [86] F. A. Shaikh and A. Ozakin, “Stability analysis of ion motion in asymmetric planar ion traps,” *J. Appl. Phys.*, vol. 112, no. 7, p. 074904, Oct. 2012.

- [87] A. Sørensen and K. Mølmer, "Entanglement and quantum computation with ions in thermal motion," *Phys. Rev. A - At. Mol. Opt. Phys.*, vol. 62, no. 2, p. 11, 2000.
- [88] D. Leibfried, R. Blatt, C. Monroe, and D. Wineland, "Quantum dynamics of single trapped ions," *Rev. Mod. Phys.*, vol. 75, no. 1, pp. 281–324, Mar. 2003.
- [89] T. G. Ballance, J. F. Goodwin, B. Nichol, L. J. Stephenson, C. J. Ballance, and D. M. Lucas, "A short response time atomic source for trapped ion experiments," *Rev. Sci. Instrum.*, vol. 89, no. 5, pp. 1–5, 2018.
- [90] M. Johanning *et al.*, "Resonance-enhanced isotope-selective photoionization of YbI for ion trap loading," *Appl. Phys. B Lasers Opt.*, vol. 103, no. 2, pp. 327–338, 2011.
- [91] Stig Stenholm, "The semiclassical theory of laser cooling," *Rev. Mod. Phys.*, vol. 58, no. 3, pp. 699–, 1986.
- [92] E. Mount *et al.*, "Single qubit manipulation in a microfabricated surface electrode ion trap," *New J. Phys.*, vol. 15, 2013.
- [93] M. Harlander, M. Brownnutt, W. Hänsel, and R. Blatt, "Trapped-ion probing of light-induced charging effects on dielectrics," *New J. Phys.*, vol. 12, 2010.
- [94] S. X. Wang, G. Hao Low, N. S. Lachenmyer, Y. Ge, P. F. Herskind, and I. L. Chuang, "Laser-induced charging of microfabricated ion traps," *J. Appl. Phys.*, vol. 110, no. 10, 2011.
- [95] S. Hong, Y. Kwon, C. Jung, M. Lee, T. Kim, and D. I. D. Cho, "A New Microfabrication Method for Ion-Trap Chips That Reduces Exposure of Dielectric Surfaces to Trapped Ions," *J. Microelectromechanical Syst.*, vol. 27, no. 1, pp. 28–30, 2018.
- [96] D. A. Hite *et al.*, "100-Fold Reduction of Electric-Field Noise in an Ion Trap Cleaned With In situ Argon-Ion-Beam Bombardment," *Phys. Rev. Lett.*, vol. 109, no. 10, pp. 1–5, 2012.
- [97] D. A. Hite *et al.*, "Surface science for improved ion traps," *MRS Bull.*, vol. 38, no. 10, pp. 826–833, Oct. 2013.
- [98] K. Y. Lin, G. H. Low, and I. L. Chuang, "Effects of electrode surface roughness on motional heating of trapped ions," *Phys. Rev. A*, vol. 94, no. 1, pp. 1–11, 2016.
- [99] R. C. Sterling, "Ytterbium ion trapping and microfabrication of ion trap arrays," University of Sussex, 2011.
- [100] M. Niedermayr *et al.*, "Cryogenic surface ion trap based on intrinsic silicon," *New J. Phys.*, vol. 16, 2014.
- [101] J. Krupka, J. Breeze, A. Centeno, N. Alford, T. Claussen, and L. Jensen, "Measurements of Permittivity, Dielectric Loss Tangent, and Resistivity of Float-Zone Silicon at Microwave Frequencies," *IEEE Trans. Microw. Theory Tech.*, vol. 54, no. 11, pp. 3995–4001, Nov. 2006.
- [102] N. D. Guise *et al.*, "Ball-grid array architecture for microfabricated ion traps," *J. Appl. Phys.*, vol. 117, no. 17, p. 174901, 2015.
- [103] A. Bautista-Salvador *et al.*, "Multilayer ion trap technology for scalable quantum computing and quantum simulation," *New J. Phys.*, vol. 21, no. 4, p. 043011, Apr. 2019.
- [104] D. T. C. Allcock *et al.*, "Heating rate and electrode charging measurements in a scalable, microfabricated, surface-electrode ion trap," *Appl. Phys. B*, vol. 107, no. 4, pp. 913–919, 2012.
- [105] R. C. Sterling, M. D. Hughes, C. J. Mellor, and W. K. Hensinger, "Increased surface flashover

voltage in microfabricated devices," *Appl. Phys. Lett.*, vol. 103, no. 14, p. 143504, Sep. 2013.

- [106] S. Ragg, C. Decaroli, T. Lutz, and J. P. Home, "Segmented ion-trap fabrication using high precision stacked wafers," *Rev. Sci. Instrum.*, vol. 90, no. 10, p. 103203, Oct. 2019.
- [107] A. M. Eltony, S. X. Wang, G. M. Akselrod, P. F. Herskind, and I. L. Chuang, "Transparent ion trap with integrated photodetector," *Appl. Phys. Lett.*, vol. 102, no. 5, pp. 4–7, 2013.
- [108] C. L. Arrington *et al.*, "Micro-fabricated stylus ion trap," *Rev. Sci. Instrum.*, vol. 84, no. 8, 2013.
- [109] S. C. Doret *et al.*, "Controlling trapping potentials and stray electric fields in a microfabricated ion trap through design and compensation," *New J. Phys.*, vol. 14, 2012.
- [110] G. R. Brady *et al.*, "Integration of fluorescence collection optics with a microfabricated surface electrode ion trap," *Appl. Phys. B*, vol. 103, no. 4, pp. 801–808, Jun. 2011.
- [111] R. Dubessy, T. Coudreau, and L. Guidoni, "Electric field noise above surfaces: A model for heating-rate scaling law in ion traps," *Phys. Rev. A - At. Mol. Opt. Phys.*, vol. 80, no. 3, pp. 1–4, 2009.
- [112] A. Safavi-Naini, P. Rabl, P. F. Weck, and H. R. Sadeghpour, "Microscopic model of electric-field-noise heating in ion traps," *Phys. Rev. A - At. Mol. Opt. Phys.*, vol. 84, no. 2, pp. 1–7, 2011.
- [113] R. G. DeVoe and C. Kurtsiefer, "Experimental study of anomalous heating and trap instabilities in a microscopic Ba-137 ion trap," *Phys. Rev. A - At. Mol. Opt. Phys.*, vol. 65, no. 6, p. 8, 2002.
- [114] L. Deslauriers, S. Olmschenk, D. Stick, W. K. Hensinger, J. Sterk, and C. Monroe, "Scaling and suppression of anomalous heating in ion traps," *Phys. Rev. Lett.*, vol. 97, no. 10, pp. 1–4, 2006.
- [115] M. Brownnutt, M. Kumph, P. Rabl, and R. Blatt, "Ion-trap measurements of electric-field noise near surfaces," *Rev. Mod. Phys.*, vol. 87, no. 4, 2015.
- [116] J. A. Sedlacek *et al.*, "Distance scaling of electric-field noise in a surface-electrode ion trap," *Phys. Rev. A*, vol. 97, no. 2, p. 020302, Feb. 2018.
- [117] I. A. Boldin, A. Kraft, and C. Wunderlich, "Measuring Anomalous Heating in a Planar Ion Trap with Variable Ion-Surface Separation," *Phys. Rev. Lett.*, vol. 120, no. 2, p. 23201, 2018.
- [118] C. D. Bruzewicz, J. M. Sage, and J. Chiaverini, "Measurement of ion motional heating rates over a range of trap frequencies and temperatures," *Phys. Rev. A - At. Mol. Opt. Phys.*, vol. 91, no. 4, pp. 1–6, 2015.
- [119] R. McConnell, C. Bruzewicz, J. Chiaverini, and J. Sage, "Reduction of trapped-ion anomalous heating by in situ surface plasma cleaning," *Phys. Rev. A - At. Mol. Opt. Phys.*, vol. 92, no. 2, pp. 1–5, 2015.
- [120] A. M. Eltony, H. G. Park, S. X. Wang, J. Kong, and I. L. Chuang, "Motional heating in a graphene-coated ion trap," *Nano Lett.*, vol. 14, no. 10, pp. 5712–5716, 2014.
- [121] D. A. Hite, K. S. McKay, S. Kotler, D. Leibfried, D. J. Wineland, and D. P. Pappas, "Measurements of trapped-ion heating rates with exchangeable surfaces in close proximity," *MRS Adv.*, vol. 2, no. 41, pp. 2189–2197, Jan. 2017.
- [122] E. Kim *et al.*, "Electric-field noise from carbon-adatom diffusion on a Au(110) surface: First-principles calculations and experiments," *Phys. Rev. A*, vol. 95, no. 3, pp. 1–8, 2017.

- [123] J. A. Sedlacek *et al.*, “Evidence for multiple mechanisms underlying surface electric-field noise in ion traps,” *Phys. Rev. A*, vol. 98, no. 6, p. 063430, Dec. 2018.
- [124] C. Noel *et al.*, “Electric-field noise from thermally activated fluctuators in a surface ion trap,” *Phys. Rev. A*, vol. 99, no. 6, p. 063427, Jun. 2019.
- [125] K. G. Ray, B. M. Rubenstein, W. Gu, and V. Lordi, “Van Der Waals-corrected density functional study of electric field noise heating in ion traps caused by electrode surface adsorbates,” *New J. Phys.*, vol. 21, no. 5, 2019.
- [126] K. Lakhmankiy *et al.*, “Observation of superconductivity and surface noise using a single trapped ion as a field probe,” *Phys. Rev. A*, vol. 99, no. 2, p. 023405, Feb. 2019.
- [127] S. X. Wang, Y. Ge, J. Labaziewicz, E. Dauler, K. Berggren, and I. L. Chuang, “Superconducting microfabricated ion traps,” *Appl. Phys. Lett.*, vol. 97, no. 24, 2010.
- [128] M. Kumph, C. Henkel, P. Rabl, M. Brownnutt, and R. Blatt, “Electric-field noise above a thin dielectric layer on metal electrodes,” *New J. Phys.*, vol. 18, no. 2, p. 023020, Feb. 2016.
- [129] A. Grounds, “Cryogenic technologies for scalable trapped ion quantum computing .,” University of Sussex, 2018.
- [130] F. Mintert and C. Wunderlich, “Ion-Trap Quantum Logic Using Long-Wavelength Radiation,” *Phys. Rev. Lett.*, vol. 87, no. 25, p. 257904, Nov. 2001.
- [131] S. Weidt *et al.*, “Trapped-Ion Quantum Logic with Global Radiation Fields,” *Phys. Rev. Lett.*, vol. 117, no. 22, pp. 1–6, 2016.
- [132] C. Ospelkaus *et al.*, “Microwave quantum logic gates for trapped ions,” *Nature*, vol. 476, no. 7359, pp. 181–184, 2011.
- [133] T. P. Harty, M. A. Sepiol, D. T. C. Allcock, C. J. Ballance, J. E. Tarlton, and D. M. Lucas, “High-Fidelity Trapped-Ion Quantum Logic Using Near-Field Microwaves,” *Phys. Rev. Lett.*, vol. 117, no. 14, pp. 1–6, 2016.
- [134] A. Khromova *et al.*, “Designer spin pseudomolecule implemented with trapped ions in a magnetic gradient,” *Phys. Rev. Lett.*, vol. 108, no. 22, pp. 1–5, 2012.
- [135] K. Lake, S. Weidt, J. Randall, E. D. Standing, S. C. Webster, and W. K. Hensinger, “Generation of spin-motion entanglement in a trapped ion using long-wavelength radiation,” *Phys. Rev. A*, vol. 91, no. 1, p. 012319, Jan. 2015.
- [136] Y. Kawai, K. Shimizu, A. Noguchi, S. Urabe, and U. Tanaka, “Surface-electrode trap with an integrated permanent magnet for generating a magnetic-field gradient at trapped ions,” *J. Phys. B At. Mol. Opt. Phys.*, vol. 50, no. 2, p. 025501, Jan. 2017.
- [137] S. X. Wang, J. Labaziewicz, Y. Ge, R. Shewmon, and I. L. Chuang, “Individual addressing of ions using magnetic field gradients in a surface-electrode ion trap,” *Appl. Phys. Lett.*, vol. 94, no. 9, 2009.
- [138] M. Carsjens, M. Kohnen, T. Dubielzig, and C. Ospelkaus, “Surface-electrode Paul trap with optimized near-field microwave control,” *Appl. Phys. B Lasers Opt.*, vol. 114, no. 1–2, pp. 243–250, 2014.
- [139] R. Srinivas *et al.*, “Trapped-Ion Spin-Motion Coupling with Microwaves and a Near-Motional Oscillating Magnetic Field Gradient,” *Phys. Rev. Lett.*, vol. 122, no. 16, p. 163201, Apr. 2019.
- [140] J. Welzel, F. Stopp, and F. Schmidt-Kaler, “Spin and motion dynamics with zigzag ion crystals

in transverse magnetic gradients,” *J. Phys. B At. Mol. Opt. Phys.*, vol. 52, no. 2, p. 025301, Jan. 2019.

- [141] M. Drndić, K. S. Johnson, J. H. Thywissen, M. Prentiss, and R. M. Westervelt, “Microelectromagnets for atom manipulation,” *Appl. Phys. Lett.*, vol. 72, no. 22, pp. 2906–2908, 1998.
- [142] R. Folman, P. Kröger, D. Cassettari, B. Hessmo, T. Maier, and J. Schmiedmayer, “Controlling cold atoms using nanofabricated surfaces: Atom chips,” *Phys. Rev. Lett.*, vol. 84, no. 20, pp. 4749–4752, 2000.
- [143] W. Hänsel, P. Hommelhoff, T. W. Hänsch, and J. Reichel, “Bose–Einstein condensation on a microelectronic chip,” *Nature*, vol. 413, no. 6855, pp. 498–501, Oct. 2001.
- [144] R. Folman, P. Krüger, J. Schmiedmayer, J. Denschlag, and C. Henkel, “Microscopic Atom Optics: From Wires to an Atom Chip,” *Adv. At. Mol. Opt. Phys.*, vol. 48, no. C, pp. 263–356, 2002.
- [145] T. H. Kim, P. F. Herskind, and I. L. Chuang, “Surface-electrode ion trap with integrated light source,” *Appl. Phys. Lett.*, vol. 98, no. 21, pp. 1–4, 2011.
- [146] K. K. Mehta, C. D. Bruzewicz, R. McConnell, R. J. Ram, J. M. Sage, and J. Chiaverini, “Integrated optical addressing of an ion qubit,” *Nat. Nanotechnol.*, vol. 11, no. 12, pp. 1066–1070, 2016.
- [147] K. K. Mehta and R. J. Ram, “Precise and diffraction-limited waveguide-to-free-space focusing gratings,” *Sci. Rep.*, vol. 7, no. 1, pp. 1–8, 2017.
- [148] R. J. Niffenegger *et al.*, “Integrated optical control and enhanced coherence of ion qubits via multi-wavelength photonics,” pp. 1–9, 2020.
- [149] K. K. Mehta, C. Zhang, M. Malinowski, T.-L. Nguyen, M. Stadler, and J. P. Home, “Integrated optical multi-ion quantum logic,” 2020.
- [150] S. Crain, E. Mount, S. Baek, and J. Kim, “Individual addressing of trapped $^{171}\text{Yb}^+$ ion qubits using a microelectromechanical systems-based beam steering system,” *Appl. Phys. Lett.*, vol. 105, no. 18, pp. 1–5, 2014.
- [151] J. T. Merrill *et al.*, “Demonstration of integrated microscale optics in surface-electrode ion traps,” *New J. Phys.*, vol. 13, 2011.
- [152] M. Ghadimi *et al.*, “Scalable ion–photon quantum interface based on integrated diffractive mirrors,” *npj Quantum Inf.*, vol. 3, no. 1, p. 4, 2017.
- [153] P. F. Herskind, S. X. Wang, M. Shi, Y. Ge, M. Cetina, and I. L. Chuang, “Microfabricated surface ion trap on a high-finesse optical mirror,” *Opt. Lett.*, vol. 36, no. 16, p. 3045, Aug. 2011.
- [154] A. Van Rynbach, P. Maunz, and J. Kim, “An integrated mirror and surface ion trap with a tunable trap location,” *Appl. Phys. Lett.*, vol. 109, no. 22, 2016.
- [155] H. Takahashi, E. Kassa, C. Christoforou, and M. Keller, “Strong Coupling of a Single Ion to an Optical Cavity,” *Phys. Rev. Lett.*, vol. 124, no. 1, p. 013602, Jan. 2020.
- [156] S. Crain *et al.*, “High-speed low-crosstalk detection of a $^{171}\text{Yb}^+$ qubit using superconducting nanowire single photon detectors,” *Commun. Phys.*, vol. 2, no. 1, p. 97, Dec. 2019.
- [157] D. Kielpinski, C. Volin, E. W. Streed, F. Lenzini, and M. Lobino, “Integrated optics architecture for trapped-ion quantum information processing,” *Quantum Inf. Process.*, vol. 15, no. 12, pp. 5315–5338, 2016.

- [158] R. Bowler, U. Warring, J. W. Britton, B. C. Sawyer, and J. Amini, "Arbitrary waveform generator for quantum information processing with trapped ions," *Rev. Sci. Instrum.*, vol. 84, no. 3, 2013.
- [159] K. G. Johnson *et al.*, "Active stabilization of ion trap radiofrequency potentials," *Rev. Sci. Instrum.*, vol. 87, no. 5, p. 053110, May 2016.
- [160] R. C. Sterling, M. D. Hughes, C. J. Mellor, and W. K. Hensinger, "Increased surface flashover voltage in microfabricated devices," *Appl. Phys. Lett.*, vol. 103, no. 14, p. 143504, Sep. 2013.
- [161] J. D. Siverns, L. R. Simkins, S. Weidt, and W. K. Hensinger, "On the application of radio frequency voltages to ion traps via helical resonators," *Appl. Phys. B Lasers Opt.*, vol. 107, no. 4, pp. 921–934, 2012.
- [162] K. G. Johnson *et al.*, "Active stabilization of ion trap radiofrequency potentials," *Rev. Sci. Instrum.*, vol. 87, no. 5, 2016.
- [163] D. Gandolfi, M. Niedermayr, M. Kumph, M. Brownnutt, and R. Blatt, "Compact radiofrequency resonator for cryogenic ion traps," *Rev. Sci. Instrum.*, vol. 83, no. 8, 2012.
- [164] A. Detti, M. De Pas, L. Duca, E. Perego, and C. Sias, "A compact radiofrequency drive based on interdependent resonant circuits for precise control of ion traps," *Rev. Sci. Instrum.*, vol. 90, no. 2, p. 023201, Feb. 2019.
- [165] L. Daniel, C. R. Sullivan, and S. R. Sanders, "Design of microfabricated inductors," *IEEE Trans. Power Electron.*, vol. 14, no. 4, pp. 709–723, Jul. 1999.
- [166] B. S. Landman and R. L. Russo, "On a Pin Versus Block Relationship For Partitions of Logic Graphs," *IEEE Trans. Comput.*, vol. C-20, no. 12, pp. 1469–1479, Dec. 1971.
- [167] D. P. Franke, J. S. Clarke, L. M. K. Vandersypen, and M. Veldhorst, "Rent's rule and extensibility in quantum computing," *Microprocess. Microsyst.*, vol. 67, pp. 1–7, Jun. 2019.
- [168] D. Coyne, "LIGO Vacuum Compatible Materials List," *Ligo Dcc*, pp. 1–15, 2014.
- [169] S. Murali and N. Srikanth, "Acid Decapsulation of Epoxy Molded IC," *IEEE Trans. Electron. Packag. Manuf.*, vol. 29, no. 3, pp. 179–183, 2006.
- [170] I. D. Conway Lamb *et al.*, "A FPGA-based instrumentation platform for use at deep cryogenic temperatures," *Rev. Sci. Instrum.*, vol. 87, no. 1, pp. 1–8, 2016.
- [171] J. Li, T. Mattila, and V. Vuorinen, "MEMS Reliability," in *Handbook of Silicon Based MEMS Materials and Technologies: Second Edition*, Elsevier Inc., 2015, pp. 744–763.
- [172] W. Reinert, A. Kulkarni, V. Vuorinen, and P. Merz, "Metallic Alloy Seal Bonding," in *Handbook of Silicon Based MEMS Materials and Technologies: Second Edition*, Elsevier Inc., 2015, pp. 626–639.
- [173] K. Henttinen and T. Suni, "Silicon Direct Bonding," in *Handbook of Silicon Based MEMS Materials and Technologies: Second Edition*, Elsevier Inc., 2015, pp. 591–598.
- [174] A. C. Lapadatu and H. Jakobsen, "Anodic Bonding," in *Handbook of Silicon Based MEMS Materials and Technologies: Second Edition*, Elsevier Inc., 2015, pp. 599–610.
- [175] E. G. Colgan *et al.*, "A practical implementation of silicon microchannel coolers for high power chips," *IEEE Trans. Components Packag. Technol.*, vol. 30, no. 2, pp. 218–225, 2007.
- [176] R. A. Riddle and A. F. Bernhardt, "The Microchannel Heatsink with Liquid Nitrogen Cooling," *High Heat Flux Eng.*, vol. 1739, pp. 51–59, Feb. 1993.

- [177] C. J. Glassbrenner and G. A. Slack, "Thermal conductivity of silicon and germanium from 3°K to the melting point," *Phys. Rev.*, vol. 134, no. 4A, 1964.
- [178] F. Sebastiano *et al.*, "Cryogenic CMOS interfaces for quantum devices," *Proc. - 2017 7th Int. Work. Adv. Sensors Interfaces, IWASI 2017*, pp. 59–62, 2017.
- [179] S. J. Pauka *et al.*, "A Cryogenic Interface for Controlling Many Qubits," pp. 1–7, 2019.
- [180] H. Jun *et al.*, "HBM (High bandwidth memory) DRAM technology and architecture," *2017 IEEE 9th Int. Mem. Work. IMW 2017*, pp. 2–5, 2017.
- [181] P. Dixit and K. Henttinen, "Via Technologies for MEMS," in *Handbook of Silicon Based MEMS Materials and Technologies: Second Edition*, Elsevier Inc., 2015, pp. 694–712.
- [182] T. R. Tan *et al.*, "Multi-element logic gates for trapped-ion qubits," *Nature*, vol. 528, no. 7582, pp. 380–383, 2015.
- [183] I. V. Inlek, C. Crocker, M. Lichtman, K. Sosnova, and C. Monroe, "Multispecies Trapped-Ion Node for Quantum Networking," *Phys. Rev. Lett.*, vol. 118, no. 25, pp. 1–5, 2017.
- [184] S. Muralidharan, S. Santra, L. Jiang, C. Monroe, and V. S. Malinovsky, "Quantum Repeaters Based on Two-Species Trapped Ions," *IEEE Photonics Soc. Summer Top. Meet. Ser. SUM 2018*, p. 109, 2018.
- [185] V. Negnevitsky, M. Marinelli, K. K. Mehta, H. Y. Lo, C. Flühmann, and J. P. Home, "Repeated multi-qubit readout and feedback with a mixed-species trapped-ion register," *Nature*, vol. 563, no. 7732, pp. 527–531, 2018.
- [186] C. D. Bruzewicz, R. McConnell, J. Stuart, J. M. Sage, and J. Chiaverini, "Dual-species, multi-qubit logic primitives for Ca+/Sr+ trapped-ion crystals," *npj Quantum Inf.*, vol. 5, no. 1, p. 102, Dec. 2019.
- [187] A. G. Fowler, A. M. Stephens, and P. Groszkowski, "High-threshold universal quantum computation on the surface code," *Phys. Rev. A - At. Mol. Opt. Phys.*, vol. 80, no. 5, pp. 1–14, 2009.

Glossary

Fidelity - The reliability of a certain operation. For a fault tolerant quantum computer, fidelities of every single operation must be above the relevant fault-tolerant threshold e.g. 99 % for the surface code [187].

RF nil (null) – The minimum energy of the RF pseudopotential and gives the ion's position in an RF field.

MEMS – Micro-ElectroMechanical Systems are devices which combine electrical and mechanical features in a fabricated device. The feature sizes used often make the processing similar to ion traps.

CMOS – Complementary Metal Oxide Semiconductors is a material structure which is used to make digital logic circuits. It is also a mature industry which produces highly reliable structures at high quantities.

Hessian Matrix – Matrix of second order partial derivatives. In this case, derivatives of the total potential seen by the ion.

Pseudopotential – An effective potential which accounts for the ion's motion in an oscillating electric field.

PECVD – Plasma Enhanced Chemical Vapour Deposition is a method of depositing materials via chemical reaction of ionised gases.

Sputtering – A method of depositing a variety of materials onto a surface using accelerated ion into a target of said material.

Evaporation – A method of depositing metals onto a surface by evaporation a metal and the resulting flux, coating the surface.

RIE / Plasma etching – Reactive Ion Etching uses a plasma to directionally etch a material.

Breakdown – The point at which two, electrically isolated electrodes, become shorted due to a large voltage. This often damages the electrodes in the process.

CCWs – Current Carrying Wires are ion trap specific structures which are designed to use currents to generate magnetic fields.

Damascene process – A fabrication process in which a pattern is etched that is subsequently filled (such as with copper). It is then planarized using a chemical mechanical polish. The dual damascene process combines pattern and vertical connections into one fabrication process.

Numerical Aperture – A value that characterises the solid angle a sensor or light source is exposed to of an object, in this case, an ion. This is a dimensionless quantity.

Die – A cut-out piece of a larger, fabricated wafer. For integrated circuits, a die is typically packaged in an epoxy afterwards, making them incompatible with UHV environments.

Collection Efficiency – The percentage of collected photons that have been emitted by an object.

Node – An established fabrication method which uses fixed fabrication methods to create structures. These can be characterised by feature size, materials, voltages and many other aspects.

Ball grid array – A method that uses bumped balls to attach a die to a circuit.